Available online at www.sciencedirect.com
SCIENCE DIRECT®
International Journal of Heat and Mass Transfer 48 (2005) 3773–3792
International Journal of HEAT and MASS TRANSFER
www.elsevier.com/locate/ijhmt

Thermoacoustics and related oscillatory heat and fluid flows in micro heat exchangers

Philippe Nika *, Yannick Bailly [1], François Guermeur [2]

Département CREST FEMTO-ST/UMR CNRS 6174, Parc technologique, 2, avenue Jean Moulin, 90000 Belfort, France

Received 23 February 2004; received in revised form 21 December 2004

Abstract

Classical linear thermoacoustic theory is applied to compact micro heat exchangers and the validity of such calculus applied to micro scale is discussed. Expressions for the radial profiles and average values of the fluid axial velocity and temperature are demonstrated, formulations for first order friction and heat transfer coefficients of oscillating flows are deduced. It is shown how aerodynamic and thermal performances of a micro heat exchanger in pulsed flow regime can be characterized with three factors: a thermal characteristic time, an aerodynamic matrix of transfer and a thermal efficiency. The model proposed is devoted to design the micro heat exchangers of micro refrigerators dedicated to the cooling of electronic components.

Keywords: Micro heat exchangers; Thermoacoustics; Oscillating compressible flows; Friction factor; Convection coefficient; Electric scheme; Thermal efficiency

1. Introduction

In recent years, many new applications in Micro Electro Mechanical Systems (MEMS) have been developed in different scientific fields: electronics, avionics, biotechnologies, telecommunications, engineering process, etc. Most of these applications (e.g. micro electronic cooling devices) need micro heat sources/sink and/or use micro heat exchangers. In refrigeration of micro electronic components, important heat production, up to 100 W/cm^2, are currently observed and many miniaturized systems have been studied during last years for maintaining the component at a temperature as low as possible. A review of numerous works dedicated to such applications can be obtained in Refs. [1,2]. In fact, with the development of micro scale thermal, fluidic, chemical and biological systems, the realization of ultra compact heat exchangers or thermal ducts made of a juxtaposition of microchannels has become an important scope for many research institutions. The "LIGA" (Lithographie Galvano Abformung) techniques of fabrication applied to micro channels made of silicon, permits to realize very efficient compact heat exchangers actually. With such devices involving a liquid or a two-phase coolant, heat transfers are very efficient, however an electrical risk of contact between the fluid and the

* Corresponding author. Tel.: +33 03 84 57 82 04/18; fax: +33 03 84 57 00 32.
E-mail addresses: philippe.nika@univ-fcomte.fr (P. Nika), yannick.bailly@univ-fcomte.fr (Y. Bailly), francois.guermeur@univ-fcomte.fr (F. Guermeur).
[1] Tel.: +33 03 84 57 82 08; fax: +33 03 84 57 00 32.
[2] Tel.: +33 03 84 57 82 08; fax: +33 03 84 57 00 32.

0017-9310/$ - see front matter © 2005 Elsevier Ltd. All rights reserved.
doi:10.1016/j.ijheatmasstransfer.2005.02.006

Nomenclature

a	thermal diffusivity
a, b, c, d	thermoacoustic matrix
B_T	velocity source term Eq. (74)
Bi	Biot number Eq. (98)
c	sound celerity
c_g	mass heat capacity
C_f	friction factor Eq. (31)
C_T	sound propagation constant Eq. (76)
C_U	compliance per unit length Eq. (72)
C_{plxden}, C_{plx12}	complex number Eqs. (63) and (64)
d	distance between fins
disp	gaz displacement
d_h	hydraulic diameter
D_1, D_1', D_2, D_2'	constants Eqs. (A8)–(A10)
e	thickness
E	exchanger efficiency
f	frequency
$f_{0\eta}$	Math function Eq. (17)
g_0	Math function Eq. (19)
h	convection heat coefficient Eq. (34)
H_x, h_x	enthalpic flux density at x
$\Im$	imaginary part
j	complex imaginary
k	thermal conductivity
Kn	Knudsen number Eq. (1)
K_p	permeability Eq. (43)
l_0, l, $\bar{l}$	exchanger length, plates distance, mean free path
L_{Ux}	inductance for unit length
$\dot{m}$	mass flow rate
$\overline{M}$	molar mass
N	fin number
Nu	Nusselt number Eq. (36)
P, p	pressure
Pr	Prandtl number Eq. (4)
$\dot{Q}$	axial thermal energy power
r	mass thermodynamic gas constant
r_{Ux}, r_T	resistance for unit length, viscous, thermal
$\Re$	real part
$\overline{R}$	molar thermodynamic constant
Re	Reynolds number Eq. (32)
S	sections Eq. (57)
s, s^g, s^t	Stokes/Womersley numbers Eqs. (5) and (15)
t	time
T	temperature
u, v	axial, tangential velocities
$\dot{W}$	acoustical axial energy
x, y	axial and lateral coordinate
X_1, X_{-1}, X_2, X_3	constants Eq. (A11)–(A14)
Y	complex hydrodynamic admittance
Z, Z'	complex hydrodynamic impedance per unit length Eqs. (21) and (83)

Greek symbols

γ	gas isentropic coefficient
δ	penetration depth Eq. (4)
μ	dynamic viscosity
ρ	density
σ	specific area Eq. (46)
τ	time constant
ω	pulsation
Λ	nondimensional ratios
λ	wavelength
η	$\eta = 2y/l$ nondimensional radius
η_s', η	fin factors Eq. in Appendix C
Φ	energy density
Δ	thermal gradient
τ	exchanger time constant Eq. (65)

Subscripts

a, $2a$	complex amplitude (first, second order)
f	fined
g, gl	gas, glass
0	initial, inlet or equilibrium
x	at axial distance x, global at x
t	for wall
ite	iterative
imp	imposed
acou	acoustic
ext	for surrounding
eq	equivalent
l_0	at the extremity, outlet
pass	for gas flow section
reg	case of a regenerator
Si	for silicon
cold	at cold extremity
hot	at hot extremity
μ	viscous
k	thermal
wall	at the wall

Superscripts

t	for modified Stokes number notation
g	for modified Stokes number notation
$\|x\|$	modulus
$\widetilde{x}$	complex conjugate
$\langle x \rangle$	time average
$\bar{x}$	radial average

electronic elements remains a problem and moreover a complementary closed loop refrigeration cycle is also necessary. Besides whatever the considered system, a thermal problem still exists for rejecting the heat extracted in order to complete the total fluid cycle. An alternative consists in using of thermoelectric coolers, but they have a low efficiency actually (<5%) and are not adapted for cooling at a low temperature. Other means for micro systems cooling include the use of Stirling, or Gifford Mac Mahon or Pulsed Tubes Refrigerators (PTR). The latter machine can be easily adapted to micro scale [3] thanks to the LIGA techniques that can be applied to realize them; here the coolant fluid is a gas (helium) in pulsed flow, so all electric problems are avoided. The main functioning conditions prevailing in such machines are: time variable pressure, mass flow rate and temperature. The design of the internal micro heat exchangers is not clearly developed in the literature. Past experiments in laboratories concerning micro channels [4,5] have shown that the flow and the heat transfer characteristics cannot be predicted with accuracy by any correlation developed for channels of conventional size, even in the case of a permanent flow regime. At micro scale, when the channels size is progressively reduced, a transition from a continuous flow with no slip at the wall, to a slip flow with a temperature jump near the walls is observed; both effects are consequences of the gas rarefaction. In that situation, Navier–Stokes equations with classical boundary layer hypothesis remain valid no longer; modifications must be considered in physical laws. Many researches have been published about this subject [1,2] and many methods have been proposed: experimental studies (friction factor and heat transfer measurements), dimensional considerations, analytical [6] and numerical calculus, fin or porous medium approaches considering heat exchangers [7]. However, not only modifications of the flow physical laws must be envisaged; indeed the conductive and the radiative heat transfer in solid [8] are also strongly influenced at small scale: different micro scale heat transfer regimes based on the characteristic lengths of the heat carriers (electrons, phonons, photons) in comparison with the device characteristic dimensions must be considered.

In oscillating compressible flows, phenomena are much more complex and have not been entirely explored yet. In the past, most investigations about heat exchanges through the fluid in periodic flow have been treated assuming many simplifications: for example, considering an incompressible flow in a duct with linear thermal profile along the wall [9]. Dae-Young Lee [10,11] study the case of an oscillating incompressible flow in a circular pipe with a sinusoidal wall temperature distribution and apply their results to the prediction of the thermally developed region of the duct (in the case of weak amplitudes of the fluid displacement). When the wall temperature is forced, the effect of a rapid step change of the wall temperature cannot expand farther than the distance swept by the fluid. For a forced heat flux, the length of the thermal transition region increases proportionally to the operating frequency and reaches an asymptotic value similar to that of the swept distance at high frequencies.

Kornhauser and Smith [12] show a phase shift exists between the heat transfer and the bulk gas-wall temperature difference and propose to introduce a complex Nusselt number (or a complex heat transfer coefficient) to take into account this phenomenon; however their work is limited to heat transfer during compression and expansion of a motionless gas. Practically, most studies reported in the literature introduce restrictive hypothesis either on the fluid motion structure (laminar, incompressible, etc.), or on the wall temperature profile (constant or linear), or on the duct geometry (simple or infinite), and also on the oscillating conditions (weak frequency, weak displacement of the fluid, etc.). These simplified studies have important applications in thermal studies of motor engine cylinder, in human blood circulation or respiration, but are still irrelevant for Stirling, PTR or other thermoacoustic devices: indeed in these systems, the temperature distributions are not linear and the fluid displacements are important. A supplementary hard difficulty appearing when studying micro heat exchangers is introduced by the presence of important axial conduction losses through the wall; if the temperature levels are similar to those observed at normal scale, the thermal gradients become very important. Consequently severe parietal heat conduction occurs reinforcing thermoacoustic effects. What is expected in the case of a heat exchanger is generally to obtain an important variation (positive or negative) of the total axial energy rate: $\langle \dot{h}_x \rangle = c_g \langle \rho_g u T_g \rangle$ (named enthalpy flux). Of course, this is achieved in facilitating energy exchanges with a second fluid flow or with the surroundings. Usually this is reached by using a finned structure to produce an important thermal exchange area. On the contrary, in the tube of a Pulsed Tube Refrigerator (PTR) or in the regenerator of a Stirling machine, a constant energy rate (respectively maximal and null enthalpy flux) is sought and moreover these devices should be perfectly adiabatic. Fig. 1 gives a representation of the axial energy flux through the different parts (heat exchangers, regenerator, pulse tube, etc.) of a Pulse Tube Refrigerator and a classical Stirling cooler. One can note these devices require important variations of $\langle \dot{h}_x \rangle$, especially in the different thermal exchangers. On the contrary, in the other parts of the refrigerators (the tubes, the regenerators, etc.), the axial energy flux has to be as constant (or null in the regenerator) as possible and this cannot be achieved if lateral heat exchange occurs (see Section 4.2). The scope of this paper concerns thermoacoustic phenomena in multi-channel heat exchangers without phase change of the fluid, a special

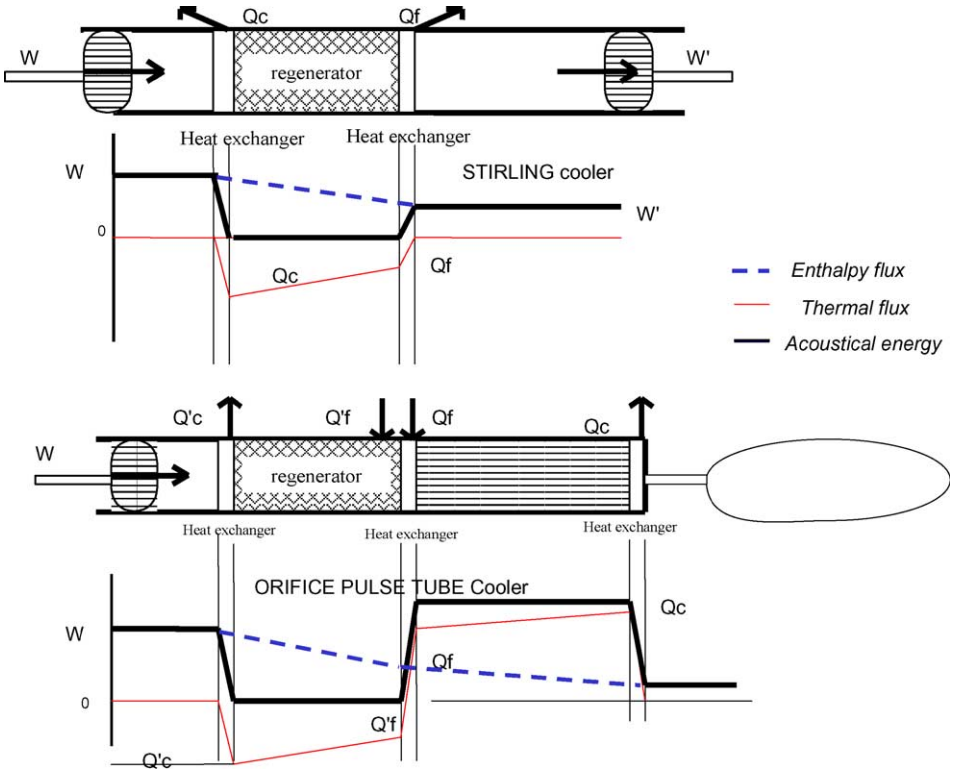

Fig. 1. Examples of energy (mechanical, thermal, enthalpy) flux evolution along a Stirling and an Orifice Pulse Tube Refrigerator.

attention being focused on micro systems. Owing to the complexity involved in this problem, some classical simplifications will be adopted. First calculus are performed for a geometry consisting of two parallel infinite plates; then the case of a micro compact heat exchanger is treated as a generalization of the previous geometry: considering average temperatures in both oscillating fluid and wall, the problem can be reduced to a one-dimensional analysis and solved eventually.

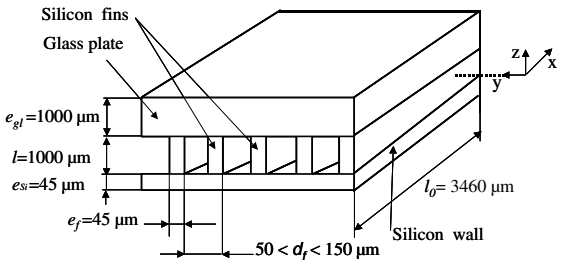

Fig. 2. Schematic representation of a micro heat exchanger made with LIGA technology.

2. Validity of usual models and hypothesis

The typical geometry of the parallel rectangular shaped channel heat exchanger under consideration is reported in Fig. 2 and a picture of such a micro system is presented in Fig. 3. As previously explained, micro-fabrication LIGA techniques allow obtaining compact heat exchangers composed of numerous fins; this ensures an important internal thermal exchange surface. Due to the silicon etching techniques used here, the minimal fins thickness "e_f" cannot be less than 50 μm while the possible gap between fins "d_f" is adjustable in a range from 50 to 150 μm. For example, the heat exchanger reported in Fig. 3 has a volume of $3.33 \times 5 \times 1$ mm and includes 60 fins made of silicon. For the type of micro canal described here, we have to examine the validity of theoretical models generally used when describing fluid flow and heat transfer, in steady as well as in dynamic unsteady regimes.

2.1. Flow classification

The Knudsen number "Kn" is the interesting parameter when examining micro systems. It is defined as the ratio between the mean free path "$\bar{l}$" of the gas molecules and a characteristic geometrical dimension of the micro device. For example, in this paper the characteristic dimension is the inter-fin distance "$d = d_f - e_f$" (see Fig. 2). So

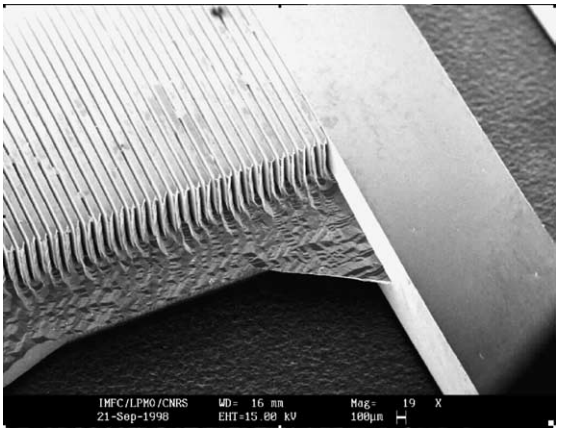

Fig. 3. Photography of a micro heat exchanger made with LIGA technology.

$$Kn = \frac{\bar{l}}{d} = \frac{\mu}{dP}\sqrt{\frac{\pi \overline{R} T}{2\overline{M}}} \tag{1}$$

For a Knudsen number $Kn < 10^{-3}$, the Navier–Stokes and the Fourier equations [13,14] remain relevant and the classical boundary conditions of no slip velocity and no temperature jump at the wall are still valid. On the contrary for Knudsen number $Kn > 0.1$, these conditions are not satisfied anymore and for greater values of Kn, the rarefied regime is observed. Taking a numerical example with slabs of thickness $e_f = 50$ μm, height $l = 1000$ μm, slab spacing $d = d_f - e_f = 100$ μm and gas helium at 1 bar, 300 K, one obtains $Kn = 3.66 \times 10^{-3}$, so the problem is near the validity limit of classical formulations. However, when increasing the gas pressure or the molecular mass of the gas "Kn" diminishes, so classical theories remain generally valid for studying problems similar to that one considered in this paper.

2.2. Thermoacoustic parameters

Four other interesting length scale parameters for thermoacoustics will be discussed below for specifying the flow classification and identifying the main important physical effects that should be carefully considered in the study.

- The ratio between the acoustic wavelength along the propagation direction and the exchanger length:

$$\Lambda_1 = \frac{\lambda}{l_0} \quad \text{with } \lambda = \frac{c}{f} = \frac{\sqrt{\gamma \overline{R} T/\overline{M}}}{f} \tag{2}$$

  where "c" is the sound velocity and "f" the oscillation frequency.

With the previous example values, and an operating frequency of 50 Hz, one obtains a wavelength: $\lambda =$ 20.3 m and a ratio $\Lambda_1 \approx 6000$; this indicates that a frequency of 30 kHz should be necessary to reach a wavelength similar to the micro exchanger length. Therefore, generally, resonance effects do not have to be considered in micro heat exchangers problems (Stirling, etc.), except of course in the case of a thermoacoustic prime mover or of a thermoacoustic cooler specially designed for taking advantage of resonance phenomena.

- The ratio between the acoustical displacement (peak to peak) and the exchanger length:

$$\Lambda_2 = \mathrm{disp}/l_0 = \frac{\bar{u}_a}{\pi f l_0} \tag{3}$$

  where $\bar{u}_a$ designates the amplitude of the acoustical velocity.

In this paper "Λ_2" is supposed to be sufficiently small so that extremities effects can be neglected in the theoretical study. Consequently, the results obtained will be restricted to the behavior of the gas particles remaining inside the heat exchanger and never leaving out. In the hypothesis of large internal displacements of the gas, as in the case of a relatively short exchanger, it is possible that a part or the totality of the gas flow crosses the system entirely. In that case, external conditions on the extremities are to be defined more accurately. Thereby, the determination of the exact behavior of the heat exchangers extremities is of great importance. This problem is difficult and has not been completely solved yet. As explained later [15], it is the thermodynamic discontinuity introduced at each extremity of the exchanger due to the material change that allows obtaining a globally nonzero heat transfer between the gas and the wall. Indeed, internal periodical thermal exchanges have globally no effect: only shuttle heat transfer occurs meaning the heat quantity exchanged when the fluid flows in one direction will be exactly balanced when it will go back in the opposite direction. This is the reason why the exchanger length must be similar to the acoustical displacement and this is in contradiction with the chosen hypothesis. Therefore in this paper the authors purpose is limited to internal thermoacoustic effects; supplementary studies will be necessary to complete the subject and particular thermodynamics effects due to non symmetry at the extremities should be studied [15]. For large values of "Λ_2", heat transfer phenomena are probably rather similar to those occurring in hydrodynamically and thermally developing region in ducts. Nevertheless, due to a general lack of knowledge concerning this specific field of research, it is not possible to answer this question accurately.

- The two ratios $\Lambda_3 = d/2\delta_\mu$ and $\Lambda'_3 = d/2\delta_k$ comparing the inter fin distance with the viscous or the thermal boundary layer thickness witch are expressed respectively by

$$\delta_\mu = \sqrt{\frac{2\mu}{\rho_g \omega}}, \quad \delta_k = \frac{\delta_\mu}{\sqrt{Pr}} \tag{4}$$

where $Pr = \frac{c_g \mu}{k_g}$ is the Prandtl number.

For rectangular channels of high shape factor and of lateral internal dimension "d", these ratios allow to quantify how the gas behavior is governed by the viscous and/or thermal boundaries induced by solid walls. Physically, "Λ_3" nearly corresponds to the nondimensional Stokes number "s" (apart from a numerical factor $1/\sqrt{2}$, see Eq. (5); sometime "s" is also named the Womersley number). In fact these parameters permit to evaluate the importance of the interaction between the acoustic wave and the wall.

$$s = \sqrt{\frac{\omega \rho_{g0} d^2}{4\mu}} = \sqrt{2}\Lambda_3 \tag{5}$$

With the conditions of the previous example, $s = 8.2 \times 10^{-2}$, while the thermal penetration depth is relatively important (1 mm): in this situation, the wall influence on the fluid flow is not negligible. Generally in thermoacoustics systems, lateral dimensions are chosen of similar size to "δ_k" in order to ensure a good coupling between the gas and the walls; this case corresponds to moderate Stokes/Womersley numbers near $s = 1$ or 2 (with both pressure and frequency higher than in the example).

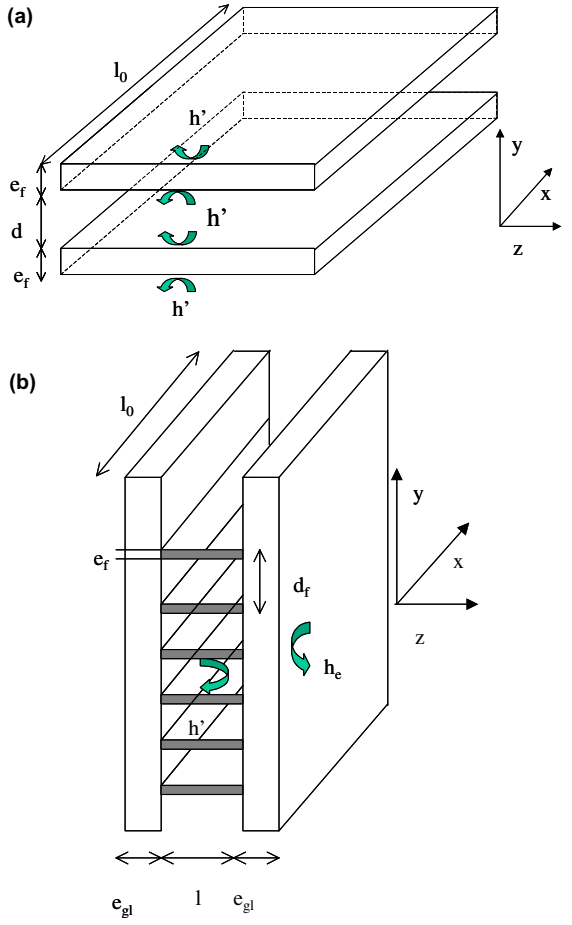

Fig. 4. (a) Simplified geometry of the parallel infinite plates heat exchanger; (b) simplified geometry of the parallel infinite plates internally finned heat exchanger.

3. Mathematical model: linear thermoacoustics

3.1. General thermoacoustics equations for two infinite parallel walls

To simplify mathematical developments, the particular case of a compressible gas flowing between two infinite parallel walls (corresponding to a high shape factor with $l_0 \gg d$) is considered. Fig. 4a presents the basic geometry. Useful equations are obtained from the classical 2D formulation [13]: mass conservation equation, momentum conservation equations, gas state equation and energy equations for the gas and the wall. The thermal gradient along the wall $\Delta_{Tx} = \mathrm{d}T_{tx}/\mathrm{d}x$ is known or imposed by an appropriate system. Boundary conditions for flow velocity and temperatures must be added to the system of general equations. Of course, as discussed in the previous chapter, the choice of these conditions depends of the global surroundings of the exchanger and also of the values of the two ratios "Kn" and "Λ_2": if the Knudsen number is important, velocity slip and temperature jump must also be taken into account.

The linear acoustic approximation is introduced into general equations: each variable is divided in an average temporal real value, depending on x and y, and the successive complex perturbation terms corresponding to the fundamental frequency (for the first order) and its successive harmonics. The secondary order term is the sum of a time dependant and of a time not dependant term; the present study will be clearly limited to the first order analysis (fundamental frequency).

$$\xi = \xi_x + \xi_a e^{j\omega t} + \xi_{2a} \quad \xi \text{ stands for } p, T_g, T_t, \rho_g \tag{6}$$

$$u = u_a e^{j\omega t} + u_{2a}, \quad v = v_a e^{j\omega t} + v_{2a}$$

Subscript a and $2a$ correspond to first and second order terms respectively. The first term in the right hand of Eq. (6) is the mean time value so it is not time dependent and it is null for the velocities (oscillating flow).

Introducing the previous hypothesis Eq. (6) in the general equations and identifying each order of the decomposition leads to a system of equations for each order:

- For the zero order system, the results are

$$\frac{\partial p_0}{\partial x} = \frac{\partial p_0}{\partial y} = 0 \tag{7}$$

$$T_{gx} = T_{tx} \tag{8}$$

and

$$\rho_{gx} = \frac{p_0}{rT_{gx}} \tag{9}$$

Eq. (7) is a proof of the average pressure uniformity in the channel. Besides in absence of acoustic wave, when the steady state is reached, the gas and the wall temperatures are identical (Eq. (8)) and they only depend on the x coordinate. The density is also uniform in a channel section and depends only on x.

- For the first order system without including extremities effects, additional simplifications are introduced:

$$\frac{\partial^2 u_a}{\partial x^2} \ll \frac{\partial^2 u_a}{\partial y^2}, \quad \frac{\partial^2 T_{ga}}{\partial x^2} \ll \frac{\partial^2 T_{ga}}{\partial y^2}, \quad \frac{\partial^2 T_{ta}}{\partial x^2} \ll \frac{\partial^2 T_{ta}}{\partial y^2}$$

These approximations assume the perturbations along the x axis to be weak in front of those occurring along the y axis. Besides this, a supplementary hypothesis for a two-dimensional flow is also introduced: $v_a \approx 0$.

So, mass and momentum first order equations lead to become

$$\begin{aligned} &\mathrm{j}\omega\rho_{ga} + u_a\frac{\partial \rho_{gx}}{\partial x} + \rho_{gx}\frac{\partial u_a}{\partial x} + \rho_{gx}\frac{\partial v_a}{\partial y} \\ &\quad \approx \mathrm{j}\omega\rho_{ga} + u_a\frac{\partial \rho_{gx}}{\partial x} + \rho_{gx}\frac{\partial u_a}{\partial x} = 0 \end{aligned} \tag{10}$$

$$\begin{aligned} &\mathrm{j}\omega\rho_{gx}u_a + \frac{\partial p_a}{\partial x} - \frac{4}{3}\mu\frac{\partial^2 u_a}{\partial x^2} - \mu\frac{\partial^2 u_a}{\partial y^2} - \frac{1}{3}\mu\frac{\partial^2 v_a}{\partial x\partial y} \\ &\quad \approx \mathrm{j}\omega\rho_{gx}u_a + \frac{\partial p_a}{\partial x} - \mu\frac{\partial^2 u_a}{\partial y^2} = 0 \end{aligned} \tag{11}$$

$$\mathrm{j}\omega\rho_{gx}v_a + \frac{\partial p_a}{\partial y} - \frac{4}{3}\mu\frac{\partial^2 v_a}{\partial y^2} - \mu\frac{\partial^2 v_a}{\partial x^2} - \frac{1}{3}\mu\frac{\partial^2 u_a}{\partial x\partial y} \approx \frac{\partial p_a}{\partial y} = 0 \tag{12}$$

The two first order energy equations become:

$$\begin{aligned} &c_g\rho_{gx}\mathrm{j}\omega T_{ga} + c_g\rho_{gx}u_a\Delta_{Tx} - \mathrm{j}\omega p_a \\ &\quad - k_g\left(\frac{\partial^2 T_{ga}}{\partial x^2} + \frac{\partial^2 T_{ga}}{\partial y^2}\right) = 0 \\ &\Rightarrow \quad \frac{\partial^2 T_{ga}}{\partial y^2} - \frac{\mathrm{j}\omega}{a_g}\frac{\rho_{gx}}{\rho_{g0}}T_{ga} + \frac{\mathrm{j}\omega}{k_g}p_a - \frac{\rho_{gx}}{\rho_{g0}}\frac{1}{a_g}u_a\Delta_{Tx} \approx 0 \end{aligned} \tag{13}$$

$$\mathrm{j}\omega T_{ta} - \frac{k_t}{\rho_t c_t}\left(\frac{\partial^2 T_{ta}}{\partial x^2} + \frac{\partial^2 T_{ta}}{\partial y^2}\right) \approx \mathrm{j}\omega T_{ta} - a_t\frac{\partial^2 T_{ta}}{\partial y^2} = 0 \tag{14}$$

3.2. Transversal evolution of the axial velocity between two infinite parallel walls

Now let us introduce two modified complex Stokes/Womersley numbers:

$$\begin{aligned} s^g &= s\sqrt{\mathrm{j}\frac{\rho_{gx}}{\rho_{g0}}} = \sqrt{2\mathrm{j}}\Lambda_3\sqrt{\frac{\rho_{gx}}{\rho_{g0}}} \quad \text{and} \\ s^t &= s\sqrt{\mathrm{j}\frac{a_{g0}}{a_t}} = \sqrt{2\mathrm{j}}\Lambda_3\sqrt{\frac{a_{g0}}{a_t}} \end{aligned} \tag{15}$$

The solving of Eq. (12), using classical boundary conditions (no slip velocity and no temperature jump at the wall), gives the lateral variation of the local axial velocity:

$$u_a(x,\eta) = \frac{\mathrm{j}}{\rho_{gx}\omega}\frac{\partial p_a}{\partial x}\left(1 - f_{0\eta}(s^g)\right) \tag{16}$$

where the mathematical functions and the nondimensional variable are [16]

$$f_{0\eta}(\xi) = \frac{Ch[\eta\xi]}{Ch[\xi]}, \quad \eta = \frac{2y}{d} \tag{17}$$

So the average axial velocity is expressed by

$$\begin{aligned} \bar{u}_a &= \frac{\mathrm{j}}{\rho_{gx}\omega}\frac{\partial p_a}{\partial x}(1 - g_0(s^g)) = u'_\infty(1 - g_0(s^g)) \\ &= -\frac{1}{Z'_{ux}}\frac{\partial p_a}{\partial x} \end{aligned} \tag{18}$$

where g_0 is a function defined by [16]

$$g_0(\xi) = \left(\frac{Th(\xi)}{\xi}\right) \tag{19}$$

$$u'_\infty = \frac{\mathrm{j}}{\rho_{gx}\omega}\frac{\partial p_a}{\partial x} \tag{20}$$

is the free velocity amplitude far from walls, and

$$Z'_{ux} = \frac{\mathrm{j}\rho_{gx}\omega}{(1 - g_0(s^g))} \tag{21}$$

is the complex acoustical impedance of the considered geometry (infinite parallel plates).

Figs. 5 and 6 show the evolutions of the "$f_{0\eta}$" and "g_0" Rott [16] complex functions versus the Stokes number "s" (quite similar to the ratio between the wall distance and the periodic boundary layer thickness Eq. (5)); other functions for different geometries including rectangular ducts can be found in [17 Swift]. These formulations are quite classical in the linear theory so we just discuss here some important consequences for

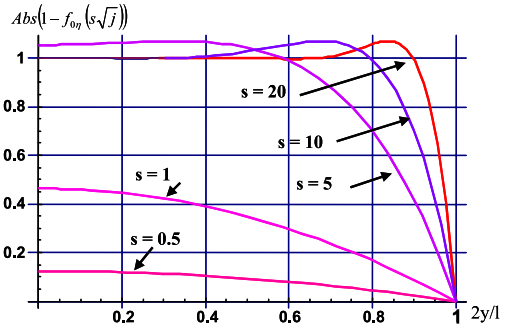

Fig. 5. Thermoacoustical mathematical function $(1 - f_0)$ versus nondimensional inter plate distance with Stokes number s as parameter.

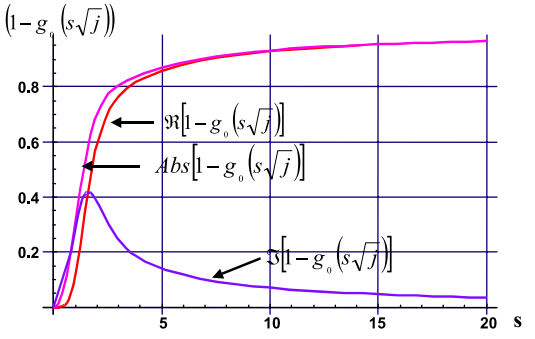

Fig. 6. Thermoacoustical mathematical function $(1 - g_0)$ versus nondimensional Stokes number s.

readers not familiar with this problem. Fig. 6 shows that for high values of "s", the imaginary part of "$1 - g_0$" vanishes meaning the average axial velocity amplitude becomes proportional to "u'_∞" and the phase lag with the pressure amplitude tends to $\pi/2$. In that case one demonstrates the wave acoustic power is null. The notation (Eq. (18)) involving the complex impedance Z'_{ux} is quite useful to model and to understand the interaction between the acoustic wave and the wall: one can clearly identify that the phase lag between pressure gradient and velocity is introduced by the wall. Remembering that "s^g" is similar to the ratio Λ_3, one concludes that for very large ducts, the phase lag between velocity and pressure fluctuations is $\pi/2$ (no interaction with wall). However, for ducts of dimensions similar to periodic boundary layer thickness, a strong coupling exists: this is the most interesting situation for thermoacoustics because the acoustic power is not null any more.

3.3. Transversal evolution of temperatures between two infinite parallel walls

Consider a particle of gas located somewhere between two parallel walls and moving in a direction parallel to the walls due to an acoustic fluctuation. The isentropic variation of its temperature is directly connected to the pressure fluctuation and can be expressed by "$p_a/c_g\rho_{gx}$". Besides, the displacement of this gas particle also due to acoustic effects is "$u'_\infty/\mathrm{j}\omega$" in the longitudinal direction. Dividing these two expressions leads to a quantity representing a kind of thermal gradient: the acoustic thermal gradient Λ_{acou},

$$\Lambda_{\mathrm{acou}} = \frac{p_a}{c_g\rho_{gx}}\mathrm{j}\omega/u'_\infty = \frac{\omega^2}{c_g}\frac{p_a}{\partial p_a/\partial x} \tag{22,23}$$

The physical signification of this variable is rather simple (see Ref. [17–21]): in an acoustic field, it represents the fluid temperature increase, independently of the surroundings. So, considering a particular gas particle (Lagrange formalism) flowing adiabatically through a temperature gradient "Λ_{Tx}" imposed by wall, its temperature variation is due to two contributions: the adiabatic fluctuation due to the pressure variation and the acoustic effect. Later, Eqs. (29) and (30), the particular case $\Lambda_{\mathrm{acou}} = \Lambda_{Tx}$ leading to a strong decrease of the global temperature variations is discussed. Substituting the acoustic gradient Eq. (23) and the velocity Eq. (16) in the gas energy equation (13) gives

$$\frac{\partial^2 T_{ga}}{\partial y^2} - \frac{\mathrm{j}\omega}{a_g}\frac{\rho_{gx}}{\rho_{g0}}T_{ga} = -\frac{\mathrm{j}\omega p_a}{k_g}\left(1 - \frac{\Lambda_{Tx}}{\Lambda_{\mathrm{acou}}}\left(1 - f_{0\eta}(s^g)\right)\right) \tag{24}$$

General solutions of Eq. (14) for wall temperature and Eq. (24) for gas temperature amplitude are calculated in Appendix A, where the new parameters X_1, X_2, X_3 are detailed; the ultimate results for temperature amplitude are

$$T_{ga} = \frac{p_a}{\rho_{gx}c_g}\left(1 - \frac{\Lambda_{Tx}}{\Lambda_{\mathrm{acou}}} + \frac{Pr}{Pr-1}\frac{\Lambda_{Tx}}{\Lambda_{\mathrm{acou}}}f_{0\eta}(s^g) - X_3 f_{0\eta}(\sqrt{Pr}s^g)\right) \tag{25}$$

and for the solid

$$T_{ta} = \frac{p_a}{\rho_{gx}c_g}\frac{1}{X_1}\left(1 + \frac{\Lambda_{Tx}}{\Lambda_{\mathrm{acou}}}\frac{1}{Pr-1} - X_3\frac{Ch(s^g)}{Ch\left(s^g\sqrt{Pr}\right)}\right) \times \left(\mathrm{Exp}\left[\eta s^g\sqrt{Pr}\right] + X_2\mathrm{Exp}\left[-\eta s^g\sqrt{Pr}\right]\right) \tag{26}$$

Generally, with the density and the heat capacity of usual materials, the temperature amplitude of the wall remains very small.

Considering expression of the coefficient X_3, in Appendix A, one can note the possible successive simplifications:

$$X_3 \to_{k_g/k_t\to 0}\left(1 + \frac{\Lambda_{Tx}}{\Lambda_{\mathrm{acou}}}\frac{1}{Pr-1}\right)\to_{\Lambda_{Tx}\to 0} 1 \tag{27}$$

So, Eq. (25) becomes

$$T_{ga} \rightarrow_{k_g/k_t \to 0} \frac{p_a}{\rho_{gx} c_g} \left(1 - f_{0\eta}(\sqrt{Pr} s^g) - \frac{\Delta_{Tx}}{\Delta_{\text{acou}}} \left(1 - \frac{Pr f_{0\eta}(s^g) - f_{0\eta}(\sqrt{Pr} s^g)}{Pr - 1} \right) \right) \quad (28)$$

The average value of the radial temperature fluctuation is similar to Eq. (25) where the function "f_0" is substituted by the function "g_0":

$$\overline{T}_{ga} = \frac{p_a}{\rho_{gx} c_g} \left(1 - \frac{\Delta_{Tx}}{\Delta_{\text{acou}}} + \frac{Pr}{Pr - 1} \frac{\Delta_{Tx}}{\Delta_{\text{acou}}} g_0(s^g) - X_3 g_0\left(s^g \sqrt{Pr}\right) \right) \quad (29)$$

If the gas thermal conductivity is small in front of that of wall, Eq. (29) leads to

$$\overline{T}_{ga} \rightarrow_{\frac{k_g}{k_t} \to 0} \frac{p_a}{\rho_{gx} c_g} \left(1 - g_0\left(s^g \sqrt{Pr}\right) - \frac{\Delta_{Tx}}{\Delta_{\text{acou}}} \left(1 - \frac{Pr g_0(s^g) - g_0(\sqrt{Pr} s^g)}{Pr - 1} \right) \right) \quad (30)$$

As explained previously Eqs. (25) or (28) prove the local or average gas temperature variations can be null during the gas displacement if the acoustic gradient Δ_{acou} (determined by the displacement and the pressure) reaches a critical value equal to the imposed gradient Δ_{Tx} in the particular case $Pr = 1$. When $X_3 = 1$, meaning the imposed gradient is negligible in front of the acoustic gradient, the gas temperature variation in the central part of the duct is quasi adiabatic and it is null at the wall. In addition, Eq. (30) also emphasizes the particular influence of the Prandtl number (Eq. (4)) on phenomena, especially on the amplitude $\overline{T}_{ga}$. Therefore fluids of low Prandtl number are generally required for thermoacoustic engines. For example, for example $Pr = 0.18$ can be obtained with Helium–Xenon mixtures [22].

4. Complex friction factor and heat transfer coefficient (first order, hypothesis of small fluctuations p_a/p_0)

4.1. Complex friction factor

By definition, the local friction factor is expressed as following:

$$C_{fx} = -\mu \frac{\partial |u_a| / \partial y|_{d/2}}{\rho_{gx} |\overline{u}_a|^2 / 2} = -\frac{2d}{Re_x} \frac{\partial |u_a| / \partial y|_{d/2}}{|\overline{u}_a| / 2} \quad (31)$$

The Reynolds number is based on the hydraulic diameter for two parallel walls: "$d_h = 2d$", this leads to Eq. (32):

$$Re_x = 2d \frac{\rho_{gx} |\overline{u}_a|}{\mu} \quad (32)$$

Combining Eqs. (16), (18) and (31), one obtains finally

$$C_{fx} Re_x = 8 \frac{s^{g^2} g_0(s^g)}{1 - g_0(s^g)} = 8 s^g \frac{Th(s^g)}{1 - \frac{Th(s^g)}{s^g}} \rightarrow_{s^g \to 0} 24 \quad (33)$$

Fig. 7 represents the evolution of the complex product "$C_f Re$" as a function of the Stokes number "s" in the case of a constant wall temperature (with $\rho_{gx}/\rho_{g0} \approx 1$). The limit of the real part of "$C_f Re$" for "s" tending to 0 is the classical value of 24, corresponding to the well known situation of two parallel infinite planes. The imaginary part of "$C_f Re$" becomes null, hence no phase lag occurs between velocity and impulsion exchange. For $s > 4$, the real and imaginary parts increase linearly and keep parallel evolutions, so the previous phase lag reaches a maximal and constant value (close to 45°). Additional results for other shapes of conduit can be deduced from functions given by Swift in [18].

4.2. Complex heat transfer coefficient

In principle, because of the nature of the oscillating flow, the global time average heat flux exchanged between the gas and the wall is null: the successive gas particles depose and load the same heat quantity from the wall as illustrated in Fig. 8a. In the particular case of a heat exchanger it is surprising that the local time average thermal exchange is null. Indeed this is in opposition with the expected effect of leading or giving a maximal heat quantity. As mentioned before, this occurs because the global thermal exchange between the gas and the walls is essentially due to the discontinuity effects at the extremities. This phenomenon justifies the reason why the length of thermal exchangers is chosen equivalent to the fluid displacement and why the ratio defined in Eq. (3) it not small. Meanwhile, during the exchange, an internal local convective heat transfer coefficient can be defined, introducing the bulk and wall temperatures difference:

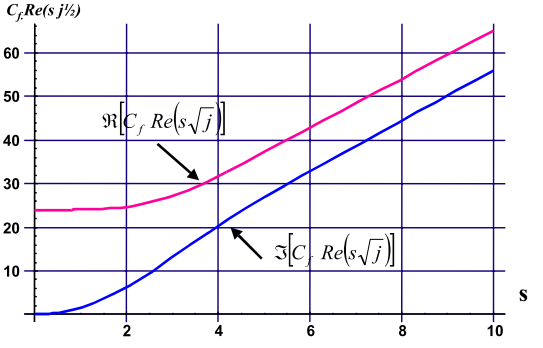

Fig. 7. Real and imaginary parts of the nondimensional product $C_f Re$ versus the Stokes numbers.

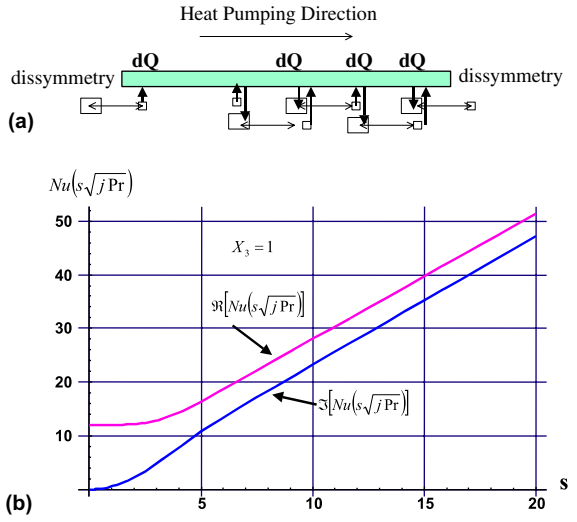

Fig. 8. (a) Illustration of the alternate heat transfer between the gas an the walls occurring in an oscillating compressible flow: null global effect of the thermal exchanges. (b) Real and imaginary parts of the nondimensional Nusselt number for instantaneous heat transfer in oscillating flow versus the Stokes number s.

$$h = k_g \frac{\left.\frac{\partial T_{ga}}{\partial y}\right|_{d/2}}{\left(\overline{T}_{ga} - T_{ta|d/2}\right)} \tag{34}$$

A calculus introducing Eqs. (25) and (26) gives the relation for "h":

$$\begin{cases} h = k_g \dfrac{2(s^g)^2 Pr}{d} \\ \quad \times \dfrac{\dfrac{g_0(s^g)}{Pr-1}\dfrac{\Delta T_x}{\Delta_{\mathrm{acou}}} - X_3 g_0\left(\sqrt{Pr}s^g\right)}{1 - \dfrac{\Delta T_x}{\Delta_{\mathrm{acou}}} + \dfrac{Pr}{Pr-1}\dfrac{\Delta T_x}{\Delta_{\mathrm{acou}}} g_0(s^g) - X_3 g_0\left(\sqrt{Pr}s^g\right) - T_{ta}|_{d/2}} \\ T_{ta}|_{d/2} = \dfrac{1}{X_1}\left(1 - \dfrac{\Delta T_x}{\Delta_{\mathrm{acou}}} + \dfrac{Pr}{Pr-1}\dfrac{\Delta T_x}{\Delta_{\mathrm{acou}}} - X_3 \dfrac{Ch(s^g)}{Ch\left(\sqrt{Pr}s^g\right)}\right) \\ \quad \times \left(e^{\sqrt{Pr}s^g} + X_2 e^{-\sqrt{Pr}s^g}\right) \end{cases} \tag{35}$$

One can deduce the complex Nusselt number expression (T_{ta} is negliged):

$$\begin{aligned} Nu &= \frac{2dh}{k_g} \\ &= 4(s^g)^2 Pr \frac{\frac{g_0(s^g)}{Pr-1}\frac{\Delta T_x}{\Delta_{\mathrm{acou}}} - X_3 g_0\left(\sqrt{Pr}s^g\right)}{1 - \frac{\Delta T_x}{\Delta_{\mathrm{acou}}} + \frac{Pr}{Pr-1}\frac{\Delta T_x}{\Delta_{\mathrm{acou}}} g_0(s^g) - X_3 g_0\left(\sqrt{Pr}s^g\right)} \\ &\to_{X_3=1;\, s\to 0} 12 \end{aligned} \tag{36}$$

Fig. 8b represents the variations of both real and imaginary parts of Nusselt number versus Stokes number when $X_3 = 1$. The evolution of the Nusselt number is quite similar to that of "$C_f Re$", revealing a strong interaction between hydraulic and thermal phenomena. Again, the presence of a nonzero imaginary part when $s > 0$ indicates the existence of a phase lag between the thermal flux and the temperature difference between gas and wall.

The "Nu" limit when the Stokes number becomes null is 12, which is greater than the well known values corresponding to the case of a laminar permanent flow occurring between two parallel plates: $Nu = 7.51$ for constant wall temperature, and $Nu = 8.235$ for constant heat flux. This discrepancy could occur because thermal transfers without fluid displacement are somewhat different from those of permanent flow regime.

Thermoacoustics calculus with second order term in equations (6) shows that a global permanent flow can be created by the nonuniform (within the channel section) viscous effects occurring during compression and release periods. In that case, longitudinal variations of the axial energy flux $\langle \dot{h}_x \rangle$ can be obtained by considering a parietal thermal exchange due to the permanent second order term in the expression of the wall temperature (see Appendix B), so:

$$k_g \left\langle \left.\frac{\partial T_{g2}}{\partial y}\right|_{d/2} \right\rangle = \frac{\partial}{\partial x}\langle \dot{h}_x \rangle \tag{37}$$

In fact, this relation shows how tangential heat transfer induces variations of the axial energy flux.

5. Characterization of compact micro heat exchangers performances

In the previous sub sections, we discussed the thermoacoustical linear theory applied to two simple parallel infinite plates as schematized on Fig. 4a; the usual compact micro heat exchangers fabricated by means of silicon technology used in microelectronics are characterized by a great number of parallel slab (silicon) gathered between two other plates made of glass, (Fig. 2). However, for engineering applications and keeping in mind the possibility to introduce the micro exchanger in more sophisticated systems, the use of simplifications seems preferable instead of developing a global numerical 3D resolution of theoretical equations with unknown or nonrealistic boundaries and operating conditions.

5.1. Averaged one-dimensional equations system

Considering a simple rectangular canal of high shape factor (~20) as presented in Fig. 4a, the general equations [13] for the zero and the first orders are integrated along the "y" axis; the hypothesis of a weakly compressible flow is adopted (not relevant for real engines but widely used in acoustics):

$$\overline{\rho_{gx} u_a} = \bar{\rho}_{gx} \bar{u}_a \tag{38}$$

Thus, the first order momentum and energy equations are averaged (see Eqs. 11,13,14):

$$\mathrm{j}\omega\bar{\rho}_{gx}\bar{u}_\mathrm{a} + \frac{\partial p_a}{\partial x} - \mu\frac{2}{l}\left.\frac{\partial u_a}{\partial y}\right|_{d/2} = 0 \tag{39}$$

$$c_g\bar{\rho}_{gx}\mathrm{j}\omega\overline{T}_{ga} + c_g\rho_{gx}\bar{u}_\mathrm{a}\Delta_{Tx} - k_g\frac{\partial^2\overline{T}_{ga}}{\partial x^2} - \mathrm{j}\omega p_a - \sigma_1 k_g\left.\frac{\partial T_{ga}}{\partial y}\right|_{d/2} = 0 \tag{40}$$

$$\mathrm{j}\omega\overline{T}_{ta} - \frac{k_t}{\rho_t c_t}\frac{\partial^2\overline{T}_{ta}}{\partial x^2} + \left.\frac{k_t}{\rho_t c_t}\sigma_2\frac{\partial T_{ta}}{\partial y}\right|_{d/2} - \left.\frac{k_t}{\rho_t c_t}\sigma_2\frac{\partial T_{ta}}{\partial y}\right|_{ef/2+d/2} = 0 \tag{41}$$

A first adaptation is applied to the momentum equation Eq. (39), introducing the apparent local permeability "K_p" instead of the velocity gradient at the wall:

$$\mathrm{j}\omega\bar{\rho}_{gx}\bar{u}_\mathrm{a} + \frac{\partial p_a}{\partial x} + \frac{\mu}{K_{px}}\bar{u}_\mathrm{a} = 0 \tag{42}$$

In the case of two infinite plates the apparent local permeability "K_{px}" is defined by

$$K_{px} = \frac{dd_h}{C_{fx}Re_x} \tag{43}$$

Only the real part of the friction factor "C_{fx}" (which was defined previously by Eq. (31)) has a physical meaning, in the case of two infinite plates for example, "$C_{fx}Re_x$" (also called Darcy product) is given by Eq. (33). Strictly, "K_{px}" as "Re_x" and "C_{fx}" depend on the "x" coordinate and the time; this induces dramatic complications of the problem, therefore the use of average constant values along the micro heat exchanger will be assumed for achieving calculations.

Eq. (42), concerning average velocity, is rewritten with the more technical form of Eq. (18):

$$\bar{u}_\mathrm{a} = -\frac{1}{Z_{Ux}}\frac{\mathrm{d}p_a}{\mathrm{d}x} \tag{44}$$

where

$$Z_{Ux} = \mathrm{j}\omega\bar{\rho}_{gx} + \frac{\mu_g}{K_{px}} = \mathrm{j}\omega L_{Ux} + r_{Ux} \tag{45}$$

"Z_{Ux}" is the complex acoustic impedance by length unit (for velocity) of the heat exchanger which is similar to Eq. (21) established in the case of two single parallel infinite plates. The first term of the right member L_{Ux} corresponds to an inductance, the second r_{Ux} to a flowing resistance.

Besides, in the temperature equations (40) and (41), due to the integration and averaging along the "y" direction, the factors depending upon the plates spacing distance "d" and upon the wall thickness "e_f" appear in several terms corresponding to specific areas defined as following:

$$\sigma_1 = \frac{2}{d} = \frac{\text{internal exchange area}}{\text{internal gas volume}}$$
$$\sigma_2 = \frac{2}{e_\mathrm{f}} = \frac{\text{internal exchange area}}{\text{wall volume}} \tag{46}$$

In principle, in Eqs. (40) and (41), the real part of the thermal flux at the boundaries (the spatial derivatives) should be substituted using a linear formulation such Eq. (34). So introducing the convective complex coefficients [12] "h" at the internal side of walls, the real part of the parietal thermal flux is expressed by

$$k_g\Re\left[\left.\frac{\partial T_g}{\partial y}\right|_{d/2}\right] = \Re[h]\Re[\overline{T}_t - \overline{T}_g] - \Im[h]\Im[\overline{T}_t - \overline{T}_g] \tag{47}$$

In the case of harmonic temperatures, one easily demonstrates that [12]

$$\Im[\overline{T}_t - \overline{T}_g] = \frac{1}{\omega}\frac{\mathrm{d}}{\mathrm{d}t}\Re[\overline{T}_t - \overline{T}_g] \tag{48}$$

So, omitting to write the symbol for real part (only measurable value) of the temperature, the expression of the oscillating thermal flux at the wall is

$$k_g\left.\frac{\partial T_g}{\partial y}\right|_{d/2} = k_t\left.\frac{\partial T_t}{\partial y}\right|_{d/2} = \Re[h](\overline{T}_t - \overline{T}_g) - \frac{\Im[h]}{\omega}\frac{\mathrm{d}\left((\overline{T}_t - \overline{T}_g)\right)}{\mathrm{d}t} \tag{49}$$

For the first order equations, if the Stokes number is weak (remember the value is $s = 0.082$ for the micro exchanger considered in the example of part 2), the imaginary part of the convective complex coefficient "h" is near 0 and the thermal flux has no noticeable phase lag with the temperature difference ($h \approx \Re[h]$, see Fig. 8b). Finally, the spatial derivations are

$$k_g\left.\frac{\partial T_{ga}}{\partial y}\right|_{d/2} = k_t\left.\frac{\partial T_{ta}}{\partial y}\right|_{d/2} = h(\overline{T}_{ta} - \overline{T}_{ga}) \tag{50}$$

$$k_t\left.\frac{\partial T_{ta}}{\partial y}\right|_{e_\mathrm{f}/2+d/2} = 0 \tag{51}$$

Introducing Eqs. (50) and (51) in temperature expression Eqs. (40) and (41), one obtains

$$\mathrm{j}\omega c_g\bar{\rho}_{gx}\overline{T}_{ga} + c_g\rho_{gx}\bar{u}_\mathrm{a}\Delta_{Tx} - k_g\frac{\partial^2\overline{T}_{ga}}{\partial x^2} - \sigma_1 h(\overline{T}_{ta} - \overline{T}_{ga}) - \mathrm{j}\omega p_a = 0 \tag{52}$$

$$\mathrm{j}\omega\overline{T}_{ta} - \frac{\sigma_2 h}{\rho_t c_t}(\overline{T}_{ga} - \overline{T}_{ta}) - \frac{k_t}{\rho_t c_t}\frac{\partial^2\overline{T}_{ta}}{\partial x^2} = 0 \tag{53}$$

Now, one needs to extrapolate the previous results Eqs. (44), (52) and (53), established for two parallels infinite plates to the limited geometry of a micro compact heat exchangers. We consider (see Fig. 4b) a whole compact heat exchanger with a great number of internal slabs, parallel to the "x,z" plane, these latter are regularly spaced along the "y" direction. To take into account of the different materials of both exchanger plates (glass) and fins (silicon), a global average thermal capacity and an average thermal conductivity in the "x" direction are introduced.

$$\rho_x c_x = \frac{\rho_f c_f e_f l + 2\rho_{gl} c_{gl} e_{gl} d_f}{e_f l + 2e_{gl} d_f} \tag{54}$$

$$k_x = \frac{k_f e_f l + 2k_{gl} e_{gl} d_f}{e_f l + 2e_{gl} d_f} \tag{55}$$

The specific areas "σ_1, σ_2" (Eq. (46)) are also modified and adapted to the realistic case: due to the thermal link between the fins and their supports, the average first order temperatures of solid material in the x plane are modified by the surroundings. For such micro heat exchangers, external heat transfer areas (plates) are currently finned and in that case a convenient finned structure factor η_s' (see definition in Appendix C) has to be introduced.

$$\sigma_1 = \frac{2Nd_f}{S_{pass}}, \quad \sigma_2 = \frac{2Nd_f}{S_x} \tag{56}$$

$$S_{pass} = Nl(d_f - e_f), \quad S_x = N(2d_f e_{gl} + le_f) \tag{57}$$

Finally a pair of one-dimensional perturbation energy equations for the gas and the equivalent solid media is considered:

$$j\omega c_g \bar{\rho}_{gx} \overline{T}_{ga} + c_g \rho_{gx} \bar{u}_a \Delta_{Tx} - k_g \frac{\partial^2 \overline{T}_{ga}}{\partial x^2} - \sigma_1 h(\overline{T}_{ta} - \overline{T}_{ga}) - j\omega p_a = 0 \tag{58}$$

$$j\omega \overline{T}_{ta} - \frac{\sigma_2 h}{\rho_x c_x}(\overline{T}_{ga} - \overline{T}_{ta}) - \frac{k_x}{\rho_x c_x} \frac{\partial^2 \overline{T}_{ta}}{\partial x^2} = 0 \tag{59}$$

5.2. Characteristic thermal time constant of the heat exchanger

Theoretically, the previous averaging technique can also be used to evaluate the axial variation of the micro exchanger temperatures in thermal static regime (at 0 order). In reality, the noninfinite dimensions and the surrounding influence dramatically change all the temperature distribution and especially averaged temperature of wall. This aspect is discussed later in this paper; for the moment, in steady conditions and neglecting the gas conductivity k_g, the following relations keep quite realistic:

$$p_0 = \text{constant}, \quad \bar{\rho}_{gx} = \frac{p_0}{r\overline{T}_{gx}}, \quad \overline{T}_{gx} = \overline{T}_{tx}$$

Thanks to the hypothesis $\frac{\partial^2 \overline{T}_{ta}}{\partial x^2} \approx 0$ and $\frac{\partial^2 \overline{T}_{ga}}{\partial x^2} \approx 0$, already assumed in Section 3 (not valid with the hypothesis Λ_2 sufficiently important), the solving of Eqs. (52) and (53) is facilitated and leads to the expressions of the average temperature amplitudes for the gas and the solid:

$$\overline{T}_{ga} = \frac{\tau_x}{\bar{\rho}_{gx} c_g}\left(j\omega p_a - c_g \bar{\rho}_{gx} \bar{u}_a \Delta_{Tx}\right) \tag{60}$$

$$\overline{T}_{ga} = \frac{j\omega p_a \tau_x}{\bar{\rho}_{gx} c_g}\left(1 - \frac{\Delta_{Tx}}{\Delta_{acou}} \frac{L_{Ux}}{Z_{Ux}}\right) \tag{61}$$

$$\overline{T}_{ta} = \sigma_2 h \frac{\left(j\omega p_a - c_g \bar{\rho}_{gx} \bar{u}_a \Delta_{Tx}\right)}{C_{plx12}} \tag{62}$$

For comfort, new notations have been introduced during the calculus:

$$C_{plxden} = \sigma_1 h + j\omega c_g \bar{\rho}_{gx} \tag{63}$$

$$C_{plx12} = j\omega \rho_x c_x \sigma_1 h - c_g \bar{\rho}_{gx}\left(\rho_x c_x \omega^2 - j\omega \sigma_2 h\right) \tag{64}$$

Previous calculus introduce in Eq. (60), a thermal time constant "τ_x", given by Eq. (65). The latter depends on the internal convective heat transfer coefficients "h", on the thermophysical equivalent material properties, c_x, ρ_x and on the specific areas σ_1, σ_2 of the compact heat exchanger. In addition, "τ_x" is a complex number, so it has a combined effect on both the module and the phase of the gas temperature amplitude.

$$\tau_x = \bar{\rho}_{gx} c_g \frac{1 + \frac{\sigma_1 \sigma_2 h^2}{C_{plx12}}}{C_{plxden}} \tag{65}$$

Eq. (61) is obtained by substitution of Eqs. (44), (22) and (45) in Eq. (60). Eq. (61), established for the compact exchanger, can be compared with the more rigorous form of Eq. (29) obtained in the case of two simple parallel infinite plates; so similar remarks are available here concerning the temperature amplitudes. The ratio between the inductance and the resistance due to viscosity effects in Z_{Ux} modifies the critical thermal gradient as ever remarked concerning the Prandtl number previously.

When examining Eqs. (65) and (61), isentropic values of the temperature variations can be observed if $h = 0$ and $s > 2$; in that case $\tau_x = -j/\omega$ is a pure imaginary. Similarly when "h" tends to infinity, "τ_x" can be expressed by Eq. (66):

$$\tau_{x(h\to\infty)} = \frac{1}{j\omega\left(1 + \frac{\rho_x c_x \sigma_1}{\bar{\rho}_{gx} c_g \sigma_2}\right)} \tag{66}$$

The positive real part and the negative imaginary part of "τ_x" indicate a phase lag always exists between the temperature and the pressure variations.

Fig. 9a and b represent respectively the evolutions of real and imaginary part of "τ" as functions of the pulsation and of the fluid velocity. The results presented concern a micro exchanger similar to that of Fig. 2 with forty silicon fins, $d_f = 150$ μm, $l_0 = 3460$ μm and with helium inflating pressure of 12 bars. When the operating frequency increases, the real part $\Re[\tau_x]$ decreases up to a constant value depending on the velocity. On the imaginary part $\Im[\tau_x]$, the velocity seems to have no influence in the studied range. The relation used here to calculate the heat transfer coefficient [23] corresponds to the thermal entry region in a rectangular channel and a boundary condition of constant heat flux:

$$h = \frac{k_g}{d_h}\left(4.36 + 1.31\left(2Re(d_h,\bar{u}_a)Pr\frac{d_h}{l_0}\right)^{0.33} \times \mathrm{Exp}\left[-13\sqrt{\frac{l_0}{2Re(d_h,\bar{u}_a)Prd_h}}\right]\right) \quad (67)$$

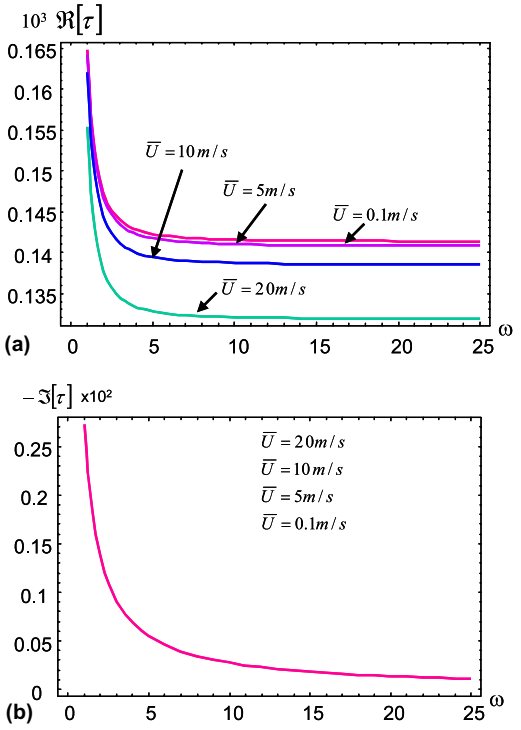

Fig. 9. (a) Real part of the thermal characteristic time τ of the heat exchanger in oscillating compressible flow versus pulsation, different axial velocities induce a variation of the heat transfer coefficient evaluated with correlation of Ref. [24]. Case Glass–Silicon micro heat exchanger $e_f = 50$ μm, $d_f = 150$ μm, $l_0 = 3460$ μm, $N = 40$ fins with helium at 12 bars. (b) Imaginary part of the thermal characteristic time τ of the heat exchanger in oscillating compressible flow versus pulsation, different axial velocities induce no observable variations. Case Glass–Silicon micro heat exchanger $e_f = 50$ μm, $d_f = 150$ μm, $l_0 = 3460$ μm, $N = 40$ fins with helium at 12 bars.

5.3. Characteristic matrix of aerodynamic transfers through the heat exchanger

From general, mass conservation and perfect gas laws averaged (in the y direction), one obtains a set of one-dimensional first order equations which are respectively:

$$j\omega\bar{\rho}_{ga} + \bar{\rho}_{gx}\frac{\partial\bar{u}_a}{\partial x} + \bar{u}_a\frac{\partial\bar{\rho}_{gx}}{\partial x} = 0 \quad (68)$$

$$\bar{\rho}_{ga} = -\frac{\bar{\rho}_{gx}}{T_{gx}}\overline{T}_{ga} + \frac{\bar{\rho}_{gx}}{p_0}p_a \quad (69)$$

Using Eq. (60) of the gas temperature amplitude:

$$\bar{\rho}_{ga} = \left(-\frac{j\omega\tau_x}{c_g T_{gx}} + \frac{\bar{\rho}_{gx}}{p_0}\right)p_a + \frac{\bar{\rho}_{gx}}{\overline{T}_{gx}}\tau_x\Delta_{Tx}\bar{u}_a \quad (70)$$

And introducing Eq. (70) into Eq. (68):

$$\frac{d\bar{u}_a}{dx} = -(j\omega C_{Ux} + 1/r_{Tx})p_a - B_{Tx}\bar{u}_a \quad (71)$$

where

$$C_{Ux} = \frac{1}{p_0}\left(1 + \frac{\gamma-1}{\gamma}\omega^2\Im[\tau_x]\right) \quad (72)$$

is the compliance per length unit of the heat exchanger;

$$1/r_{Tx} = \frac{\gamma-1}{\gamma}\frac{\omega^2}{p_0}\Re[\tau_x] \quad (73)$$

is the inverse of the thermal relaxation resistance per length unit of the heat exchanger;

$$B_{Tx} = \frac{1}{\overline{T}_{gx}}(j\omega\tau_x - 1)\Delta_{Tx} \quad (74)$$

appears as a velocity source/sink term (see Eq. (80)).

Replacing Eq. (71) into Eq. (68) leads to the Helmholtz wave equation for the pressure amplitude:

$$\frac{\partial^2 p_a}{\partial x^2} + B_{Tx}\frac{\partial p_a}{\partial x} + C_{Tx}p_a = 0 \quad (75)$$

with

$$C_{Tx} = -Z_{Ux}(j\omega C_{Ux} + 1/r_{Tx}) \quad (76)$$

Rigorously "B_{Tx}" and "C_{Tx}" depend on the axial coordinate x; it is always possible to divide the heat exchanger in a set of elementary parts of locally constant values of "B_{Tx}" and "C_{Tx}" and to connect them one after the other, however, again the use of global average values: "B_T" and "C_T" (note the new notation without x) are adopted in order to simplify the model.

If the inlet pressure variation is given Eq. (44) ("Z_u" is also a global average value):

$$x = 0 \quad p_a(0) = p_{a0}; \quad \bar{u}_a(0) = \bar{u}_{a0}; \quad \frac{\partial p_a}{\partial x}(0) = -Z_U\bar{u}_{a0} \quad (77)$$

The solution of Eq. (75) for the pressure amplitude is

$$p_a(x) = \frac{\mathrm{Exp}\left(-\frac{B_T}{2}x\right)}{\sqrt{\Delta}}\left[\left(B_T \mathrm{Sinh}\left(\sqrt{\Delta}\frac{x}{2}\right) + \sqrt{\Delta}\,\mathrm{Cosh}\left(\sqrt{\Delta}\frac{x}{2}\right)\right)p_{a0} - 2Z_U \mathrm{Sinh}\left(\sqrt{\Delta}\frac{x}{2}\right)\bar{u}_{a0}\right] \tag{78}$$

$$\Delta = B_T^2 - 4C_T \tag{79}$$

represent the wave propagation constant.

So, according to the derivative in Eq. (44), we can express the inlet conditions for the heat exchanger relatively to the outlet conditions:

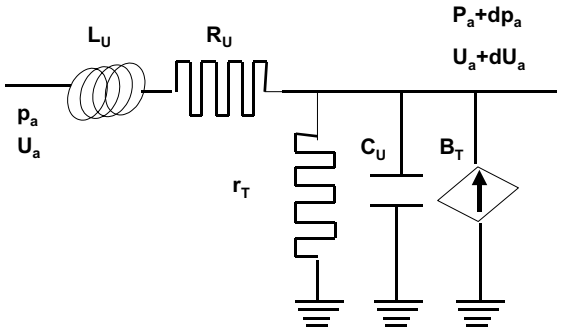

Fig. 10. Electrical equivalent scheme of a heat exchanger in oscillating compressible flow.

$$\begin{bmatrix} p_{a0} \\ \bar{u}_{a0} \end{bmatrix} = \mathrm{Exp}\left(\frac{B_T}{2}l_0\right)\begin{bmatrix} \left(-\frac{B_T}{\sqrt{\Delta}}\mathrm{Sinh}\left(\sqrt{\Delta}\frac{l_0}{2}\right) + \mathrm{Cosh}\left(\sqrt{\Delta}\frac{l_0}{2}\right)\right)\left(2\frac{Z_U}{\sqrt{\Delta}}\mathrm{Sinh}\left(\sqrt{\Delta}\frac{l_0}{2}\right)\right) \\ \left(-2\frac{C_T}{Z_U\sqrt{\Delta}}\mathrm{Sinh}\left(\sqrt{\Delta}\frac{l_0}{2}\right)\right)\left(\mathrm{Cosh}\left(\sqrt{\Delta}\frac{l_0}{2}\right) + \frac{B_T}{\sqrt{\Delta}}\mathrm{Sinh}\left(\sqrt{\Delta}\frac{l_0}{2}\right)\right) \end{bmatrix}\begin{bmatrix} p_{al_0} \\ \bar{u}_{al_0} \end{bmatrix} \tag{80}$$

Identification between Eqs. (80) and (81) permit to define the characteristic matrix of aerodynamic transfers in the micro exchanger.

$$\begin{bmatrix} p_{a0} \\ \bar{u}_{a0} \end{bmatrix} = \begin{bmatrix} a & b \\ c & d \end{bmatrix}\begin{bmatrix} p_{al_0} \\ \bar{u}_{al_0} \end{bmatrix} \tag{81}$$

Note 1: Determinant of the matrix in Eq. (80) is $\mathrm{Det} = \mathrm{Exp}(B_t l_0) \rightarrow_{\Delta_{Tx}\rightarrow 0} 1$ conformal to Eq. (74).

Note 2: If variations of "B_{Tx}" and "C_{Tx}" along the axial coordinate x has to be considered, it is possible to compute the product of the matrix of n elementary exchangers:

$$\begin{bmatrix} p_{a0} \\ \bar{u}_{a0} \end{bmatrix} = \prod_n \begin{bmatrix} a_x & b_x \\ c_x & d_x \end{bmatrix}\begin{bmatrix} p_{al_0} \\ \bar{u}_{al_0} \end{bmatrix} \tag{82}$$

Note 3: From Eqs. (18) and (71), one can represent the heat exchanger in oscillating flow functioning by its equivalent electric scheme as reported in Fig. 10. The impedances C_U, r_T and the source B_T are parallel, the impedance Z_U is series connected.

Note 4: In the particular case of an isothermal system (like a simple capillary link for example), it can be demonstrated [24] that the transfer matrix corresponds to that of a simple "PI" quadripole (as the grec letter), made of a self and a resistance series connected with two half capacities. In this way, the transfer matrix is simplified and can be expressed as following:

$$\begin{bmatrix} 1 + \frac{Z_{\mathrm{eq}}}{Y_{\mathrm{eq}}} & Z_{\mathrm{eq}} \\ \frac{1}{Y_{\mathrm{eq}}}\left(2 + \frac{Z_{\mathrm{eq}}}{Y_{\mathrm{eq}}}\right) & 1 + \frac{Z_{\mathrm{eq}}}{Y_{\mathrm{eq}}} \end{bmatrix}$$

with

$$Z_{\mathrm{eq}} = \sqrt{\frac{Z}{Y}}\mathrm{Sinh}\left(\sqrt{ZY}\right) \rightarrow_{YZ\rightarrow 0} Z$$

$$Y_{\mathrm{eq}} = \sqrt{\frac{Z}{Y}}\frac{\mathrm{Sinh}\left(\sqrt{ZY}\right)}{\mathrm{Cosh}\left(\sqrt{ZY}\right) - 1} \rightarrow_{YZ\rightarrow 0} -2/Ys \tag{83}$$

with the notation $Y = \mathrm{j}(\omega C_m + 1/r_{Tm})$.

5.4. Thermal behavior of the heat exchanger

First, the emphasis concerns internal thermal phenomena in the gas, and especially the definition of the local average internal enthalpy flux density:

$$\langle \dot{h} \rangle = c_g \langle \rho_g u T_g \rangle \tag{84}$$

We develop Eq. (84) according to Eq. (6) and take into account of the nullity of temporal average values of the axial velocity and of the mass flow rate:

$$\langle \bar{u} \rangle = 0, \quad \langle \overline{\rho_g u} \rangle = 0 \tag{85}$$

Thereby, the local enthalpy flux density representing the total energy density flowing through a unit surface, located at any x coordinate, appears as a second order quantity when averaging along a complete period:

$$\langle \dot{h}_x \rangle = c_g \langle \bar{\rho}_{gx} T_{gx} \bar{u}_a \mathrm{e}^{\mathrm{j}\omega t} + \left(\bar{\rho}_{gx} T_{gx} \bar{u}_{2a} + \bar{\rho}_{gx} \overline{T}_{ga} \bar{u}_a \mathrm{e}^{\mathrm{j}2\omega t} + \bar{\rho}_{ga} T_{gx} \bar{u}_a \mathrm{e}^{\mathrm{j}2\omega t}\right)\rangle \tag{86}$$

$$\langle \dot{h}_x \rangle \approx c_g \bar{\rho}_{gx} \langle \overline{T}_{ga} \bar{u}_a e^{j2\omega t} \rangle = c_g \bar{\rho}_{gx} \frac{1}{2} \Re\left[\overline{T}_{ga} \tilde{\bar{u}}_a\right] \tag{87}$$

Finally, substituting Eq. (60) of the temperature amplitude leads to

$$\langle \dot{h}_x \rangle = \frac{1}{2} \Re\left[\tau_x \left(j\omega p_a \tilde{\bar{u}}_a - \frac{\gamma}{\gamma - 1} \frac{p_0}{\overline{T}_{gx}} \Delta_{Tx} |\bar{u}_a|^2 \right)\right] \tag{88}$$

Now, to calculate the total axial energy flux, meaning mechanical and axial heat flux the thermal conduction through the different media must be taken into account, so

$$\dot{W}_x + \dot{Q}_x = \dot{H}_x = S_{pass} \langle \dot{h}_x \rangle - k_g S_{pass} \frac{d\overline{T}_{tx}}{dx} - k_x S_x \frac{d\overline{T}_{tx}}{dx} \tag{89}$$

Caution, $\overline{T}_{tx}$ is a global average temperature for the wall in the y,z plane for the real micro heat exchanger.

Combining Eq. (89) with Eq. (88):

$$\dot{H}_x = S_{pass} \frac{1}{2} \Re[j\omega \tau_x p_a \tilde{\bar{u}}_a] - k_{eq} S_{pass} \frac{d\overline{T}_{tx}}{dx} \tag{90}$$

with

$$k_{eq} = k_g + \frac{S_x}{S_{pass}} k_x + k_{acoux} \tag{91}$$

and

$$k_{acoux} = \frac{1}{2} \frac{\gamma}{\gamma - 1} \frac{p_0}{\overline{T}_{tx}} \Re[\tau_x] |\bar{u}_a|^2 \tag{92}$$

Eq. (92) brings out an equivalent thermoacoustical conductivity of the global system which is created by the alternative movement of the fluid particles in the ducts. As real part of "τ_x" is always positive (see Fig. 9a), one observes the effective thermal conductivity may be reinforced proportionally to both the time constant "τ_x" and the kinetic energy, hence increasing thermal losses which are particularly important in micro systems owing to important thermal gradients.

Another way to present the relation Eq. (90) is

$$\dot{H}_x = \omega S_{pass} \Im[-\tau_x] \frac{1}{2} \Re[p_a \tilde{\bar{u}}_a] - \omega S_{pass} \Re[\tau_x] \times \frac{1}{2} \Im[p_a \tilde{\bar{u}}_a] - k_{eq} S_{pass} \frac{d\overline{T}_{tx}}{dx} \tag{93}$$

Generally, $\Re[p_a \tilde{\bar{u}}_a]$ reaches an important value in traveling wave devices (Stirling, TGP), where the phase lag between velocity and pressure is small; on the contrary $\Im[p_a \tilde{\bar{u}}_a]$ is preponderant in standing wave devices (thermoacoustic refrigerators or prime movers) where the phase lag between velocity and pressure is close to 90°. Therefore in each case, imaginary part and real part of "τ_x" are fundamental data for generating a global axial energy flux. Eq. (93) (and later Eq. (94)) shows that a particular care is required when designing micro heat exchangers operating in oscillating conditions: in fact, on the contrary of classical counter flow exchangers where the thermal inertia of walls is undesirable, for thermoacoustic exchangers, a great care must be taken to obtain a nonzero value of the thermal time factor "τ_x"! (nevertheless this one must be null in a perfect thermal regenerator for example).

As mentioned previously [19, or Appendix B], axial variations of the total energy "$d\dot{H}_x$", correspond to the transversal thermal energy flux variations "$d\dot{Q}_z$", thus corresponding to the heat quantity rejected/absorbed into/by the surroundings:

$$\frac{d\dot{H}_x}{dx} = \frac{d\dot{Q}_z}{dx} = -h_e \sigma_e S_x (\overline{T}_{tx} - T_a) + N d\Phi_{ext} \tag{94}$$

The external specific surface coefficient "σ_e" given below by Eq. (95) takes into account of the finned structure with the factor "η_s'" weighting the heat transfer area (see Appendix B). Φ_{ext} is the global energy density flux received from or emitted to the surroundings by the exchanger (for example in the case of electronic component cooling, Φ_{ext} is emitted by the component).

$$\sigma_e = \frac{N d_f}{S_x}(\eta_s' + 1),$$

η_s' stands for one face with fins and

1 stands for one face without fins. (95)

If we consider a constant value of the heat exchanger time constant $\tau_x = \tau$ along the x direction, calculus (tedious and not reported here) of the derivative of Eq. (93) leads also to

$$\begin{aligned}\frac{d\dot{H}_x}{dx} = &-\frac{1}{2}\omega^2 C_U S_{pass} \Re[\tau] |p_a|^2 - \frac{1}{2}\omega \frac{1}{r_T} S_{pass} \Im[-\tau] |p_a|^2 \\ &- \frac{1}{2}\omega \Re[Z_U] \Im[-\tau] S_{pass} |\bar{u}_a|^2 + \frac{1}{2}\omega \Re[\tau] \Im[Z_U] S_{pass} |\bar{u}_a|^2 \\ &- \frac{1}{2}\omega S_{pass} \left(\omega |\tau|^2 + \Im[\tau]\right) \frac{d\,Ln(\overline{T}_{tx})}{dx} \Re[\bar{u}_a \tilde{p}_a] \\ &+ \frac{1}{2}\omega S_{pass} \Re[\tau] \frac{d\,Ln(\overline{T}_{tx})}{dx} \Im[\bar{u}_a \tilde{p}_a] - k_{eq} S_{pass} \frac{d^2 \overline{T}_{tx}}{dx^2}\end{aligned} \tag{96}$$

The first term in Eq. (96) corresponds to the energy storage in the compliance, the second term to the thermal relaxation dissipation (positive), the third term to the viscous dissipation (positive), the fourth term to an inductance effect, the fifth and sixth terms to positive or negative thermoacoustic power sources/sinks, and the last term to an equivalent global heat conduction phenomenon. The source/sink terms are directly proportional to the longitudinal temperature gradient in the wall, so they vanish if there is no gradient.

5.5. Discussion

Eqs. (94) and (96) are very important results for thermoacoustics of heat exchangers: theoretically they permit to evaluate the permanent temperature profile "T_{tx}"

along the exchanger meaning they allow estimating a global temperature of the exchanger which is the main parameter to be controlled in Stirling type machines. Nevertheless previous equations are complicated and the solutions for "T_{tx}" fundamentally depend on the boundary conditions applied to the considered exchanger; these operating conditions are not easy to be determined in experiments. For example in a thermoacoustic refrigerators, the "cold" and the "hot" exchangers are incorporated at each extremity and are in "nonperfect" thermal contact with the stack; It is similar with the regenerator of a Stirling machine. The conditions of this contact are particularly difficult to modelize, they depend of the technology adopted, the distance between the heat exchanger and the stack, difficult to optimize (high frequencies). In fact, in such devices, exchangers have to be considered as sub-elements of a more complicated system, the modelization must be global and equivalent shemes like Fig. 10 can be used. However, one has to keep in mind their specific function i.e. to create important variations of the total axial energy flux $\Delta\dot{H}_x$ facilitating absorption or rejection of transversal energy flux $\dot{Q}_z$ (see Fig. 1). Actually this is the dominant idea to keep in mind when designing such systems.

Swift [17–19] remarks a typical characteristic of thermoacoustics equations: the multiplicity of formulations that can be given and the various consequences that can be deduced. In order to obtain a form analogous to a 1D conduction equation, similar to that characterizing (for example) a slab with external losses and internal source/sink energy terms, Eqs. (94) and (96) can be equated:

$$\frac{Bi}{h_e l_0^2}\Phi(\overline{T}_{tx},x)+\frac{Bi}{l_0^2}(T_a-\overline{T}_{tx})+\frac{\partial^2\overline{T}_{tx}}{\partial x^2}=0 \tag{97}$$

Here the constant "Bi" is a Biot number:

$$Bi=\frac{h_e\sigma_e}{k_{\mathrm{eq}}}\frac{S_x}{S_{\mathrm{pass}}}l_0^2 \tag{98}$$

The first global source/sink term of Eq. (97) is deduced from Eq. (96) and easily rewritten using the form of Eq. (99) where all causes of internal heat (or cold) generation can be separated as explained above:

$$\begin{aligned}\Phi(\overline{T}_{tx},x)=&\frac{1}{2}\Re[\tau]\frac{S_{\mathrm{pass}}}{\sigma_e S_x}\frac{\omega^2|p_a|^2}{p_0}+\frac{\omega}{2}\Im[-\tau]\frac{\mu}{K_p}\frac{S_{\mathrm{pass}}}{\sigma_e S_x}|\bar{u}_{\mathrm{a}}|^2\\&-\frac{1}{2}\Re[\tau]\frac{S_{\mathrm{pass}}}{\sigma_e S_x}\bar{\rho}_g\omega^2|\bar{u}_{\mathrm{a}}|^2\\&+\frac{1}{2}\omega^2|\tau|^2\left(1+\frac{\Im[\tau]}{\omega|\tau|^2}\right)\Re[\tilde{p}_a\bar{u}_{\mathrm{a}}]\frac{S_{\mathrm{pass}}}{\sigma_e S_x}\frac{\mathrm{d}\ln[\overline{T}_{tx}]}{\mathrm{d}x}\\&-\frac{1}{2}\omega\Re[\tau]\Im[\tilde{p}_a\bar{u}_{\mathrm{a}}]\frac{S_{\mathrm{pass}}}{\sigma_e S_x}\frac{\mathrm{d}\ln[\overline{T}_{tx}]}{\mathrm{d}x}+\frac{Nd\Phi_{\mathrm{ext}}}{\sigma_e S_x}\end{aligned} \tag{99}$$

Calculus of three first terms in Eq. (99) is easy, once pressure and velocity amplitudes are known. For convenience, the equivalent electrical circuit of Section 5.3 can be used. Heat exchanger time constant "τ" may be estimated with results of Section 5.2. The main problem concern the evaluation of the two source/sink terms that are clearly depending of the axial temperature gradient itself, so an iterative method should be introduced, starting with $\mathrm{d}T_{tx}/\mathrm{d}x=0$ and modifying the latter progressively. Exact boundaries conditions are also difficult to be determined (Eqs. (97) and (99)).

In fact, different cases are possible, depending on the use of the exchanger: cold exchanger dedicated to the cooling of an electronic component which generates a heat quantity corresponding to the last term of Eq. (99) $\Phi^*=Nd\Phi_{\mathrm{ext}}/\sigma_e S_x$, or a hot exchanger built for extracting heat toward the surroundings. In the first case, the thermoacoustical terms (number three, four, five depending on the temperature profile in Eq. (99)) balance the energy dissipation (first and second terms) and the heat production Φ^*. In the second case, Φ^* does not exist and the goal is to maximize the heat exchange with the surroundings through the exchanger wall. In that second case, for example, owing to the difficulty to solve the nonlinear differential equation (97), we choose to limit mathematical development to the case of a temperature profile corresponding to a monodimensional slab which one extremity is maintained at a constant temperature "T_0", the other being insolated while considering an internal generation Φ in the slab support. In that case, this temperature profile is known as Eq. (100) and represented in Fig. 11a.

$$\frac{\overline{T}_{tx}-T_a-\Phi/h_e}{T_0-T_a-\Phi/h_e}=\frac{\mathrm{Cosh}\left(\sqrt{Bi}(1-x/l_0)\right)}{\mathrm{Cosh}\left(\sqrt{Bi}\right)} \tag{100}$$

The weaker the Biot number is, the more flat the temperature profile along the exchanger is and the higher the average temperature is. The thermal efficiency of such a heat exchanger in quasi steady state may be defined as the ratio between the thermal power exchanged and the maximal possible power exchangeable with the ambiance, so for the chosen example:

$$\begin{aligned}E&=\frac{\langle\dot{Q}\rangle}{\langle\dot{Q}_{\max}\rangle}=1-\frac{1}{l_0}\int_0^{l_0}\frac{\overline{T}_{tx}-T_a}{T_{\max}-T_a}\mathrm{d}x\\&=1-\frac{1}{\sqrt{Bi}}\frac{\mathrm{Exp}\left(2\sqrt{Bi}\right)-1}{\mathrm{Exp}\left(2\sqrt{Bi}\right)+1}\end{aligned} \tag{101}$$

Fig. 11b shows the efficiency as a function of the Biot number in the particular case $T_{\max}=T_0$; for Biot numbers greater than 400, the efficiency exceeds 0.9, whereas E decreases dramatically for Biot numbers lower than 100.

Another example concerns the set "hot exchanger-regenerator-cold exchanger" of a Pulse Tube Refrigerator devoted to electronic component cooling. For both exchangers "τ" has not to be null and the energy flux

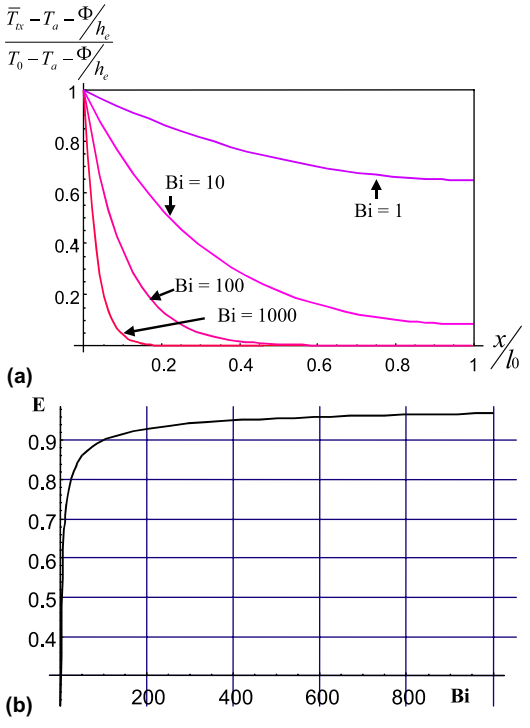

Fig. 11. (a) Temperature distribution along an equivalent slab in quasi static regime with nondimensional Biot number as parameter. (b) Efficiency of the heat exchanger versus the Biot number.

supplied by the pulsed tube is supposed to be given "$\langle \dot{H}_{\mathrm{TGP}} \rangle$". Thereby the energy density delivered by the component at the cold zone is "Φ_{ext}" and if the reverse side of the cold exchanger (length "l_{cold}") is perfectly insulated, the energy flux variation in the cold heat exchanger becomes simply Eq. (102):

$$\frac{\mathrm{d}\dot{H}_x}{\mathrm{d}x} = Nd\Phi_{\mathrm{ext}} \Rightarrow \dot{H}_x = \langle \dot{H}_{\mathrm{TGP}} \rangle - Nd\Phi_{\mathrm{ext}}(l_{\mathrm{cold}} - x) \tag{102}$$

For the "perfect adiabatic" regenerator ($\tau = 0$) (the origin $x = 0$ at the right extremity of the regenerator):

$$\frac{\mathrm{d}\dot{H}_x}{\mathrm{d}x} = 0 \Rightarrow \dot{H}_{\mathrm{reg}} = \dot{H}_{x=0} = \langle \dot{H}_{\mathrm{TGP}} \rangle - Nd\Phi_{\mathrm{ext}} l_{\mathrm{cold}} \tag{103}$$

So, Eq. (90) permits to obtain the temperature profile along the regenerator, here it is linear because of the simplifications:

$$\dot{H}_{\mathrm{reg}} = -k_{\mathrm{reg}} S_{\mathrm{reg}} \frac{\mathrm{d}T_{\mathrm{reg}}}{\mathrm{d}x} \Rightarrow T_{\mathrm{reg}} = T_{\mathrm{hot}} - x\dot{H}_{\mathrm{reg}}/k_{\mathrm{reg}} S_{\mathrm{reg}} \tag{104}$$

"T_{hot}" is imposed by the second exchanger "coupled" on the left of the regenerator, in that example.

In the ideal case of a dissipation equal to zero, the thermal conduction in the regenerator is the only cause of the energy flux, so in the considered case, the temperature profile inside the regenerator is linear and the "cold" permanent approximated temperature at the regenerator extremity is finally:

$$T_{\mathrm{cold}} = T_{\mathrm{hot}} - \frac{l_{\mathrm{reg}}}{k_{\mathrm{reg}} S_{\mathrm{reg}}} (\langle \dot{H}_{\mathrm{TGP}} \rangle - Nd l_{\mathrm{cold}} \Phi_{\mathrm{ext}}) \tag{105}$$

6. Conclusions

Linear thermoacoustics have been applied to explain thermal and aerodynamic phenomena in micro heat exchangers of planar fined geometry as those currently manufactured with LIGA techniques. The importance of the Stokes–Womersley number "s" has been exposed and especially its influence on the transversal profiles of velocity and temperature amplitudes. The notion of an acoustic thermal gradient "Δ_{acou}" has been also presented and the importance of the ratio between the thermal gradient imposed in the wall and this thermoacoustic gradient has been discussed. The temperature and velocity profiles in the case of two parallel walls are strongly depending on "f_0" and "g_0" which expressions have been detailed. Besides, the complex friction factor "C_f" and the complex thermal exchange coefficient "h" have been expressed and the authors have shown these parameters are essentially depending on the "g_0" functions of the Stokes number meaning the geometrical dimension and the operating frequency have to be taken into account simultaneously when designing such devices. Chapter 5 is devoted to the characterization of a compact micro channels heat exchanger; calculus are achieved thanks to a global model of finned structure and average formulations of energy equations. The authors propose to consider three factors: a characteristic time constant, a characteristic aerodynamic matrix transfer and the global thermal efficiency of the exchanger, all remaining convenient for oscillating flow regime.

The time constant "τ_x", a complex number, depending upon internal thermal exchanges between the gas and the walls is described as the crucial factor governing the gas average temperature amplitude. The latter values are limited by the extreme cases of isothermal and isentropic transformation, all intermediate cases remaining possible and corresponding to a particular phase lag between temperature and pressure fluctuations. Consequently "τ_x" determinates also the total energy flux "$\dot{H}_x$" through the heat exchanger.

The aerodynamic transfer matrix provides the relation of both pressure and velocity amplitudes between the exchanger extremities; its expression notably depends on the complex impedance "Z_{ux}" and admittance

"Y_U" of the exchanger and on a thermal parameter "B_T", proportional to the thermal gradient imposed along the exchanger axis and associated to a source/sink of fluid flow.

The global behaviors of the fluid through the exchanger, as well as the coupled thermal phenomena are studied by means of four important equations: Eqs. (44) and (71) for velocity amplitude and its longitudinal derivative, Eqs. (93) and (96) for the total energy flux and its derivative. A global resolution of these equations is difficult owing to the multiplicity of the various boundary conditions operating in thermoacoustic devices. Indeed, the case of a regenerator, of a stack, of a warm or a cold exchanger are very different; moreover, the study of a pure travelling wave or a standing wave is also very different. However, various source/sink energy terms have been identified in Eq. (96): sound energy consumption by thermal relaxation between the gas and the solid wall, viscous dissipation within the gas, external energy flux and thermoacoustic effect directly proportional to the temperature gradient in the solid wall.

Finally, thanks to the results of the study, a method for designing micro thermoacoustic heat exchangers has been proposed and discussed. Of course many assumptions have been used for achieving this study therefore many improvements remain possible: for example this work concerns only situations where the displacement of the fluid is considerably smaller than the length of the heat exchanger itself; Abrupt changes of the wall temperature or of the section are also prohibited. In further research, the authors intend to extend their work to short systems and to thermo-fluidic phenomena induced by strong pressure amplitude occurring in Pulse tubes or in Stirling cryocoolers.

Appendix A

Gas and wall temperatures amplitude calculus

$$\frac{\partial^2 T_{ga}}{\partial y^2} - \frac{j\omega}{a_g}\frac{\rho_{gx}}{\rho_{g0}} T_{ga} = -\frac{j\omega p_a}{k_g}\left(1 - \frac{\Delta_{Tx}}{\Delta_{\text{acou}}}(1 - f_{0\eta}(s^g))\right) \tag{A1}$$

$$j\omega T_{ta} - a_t \frac{\partial^2 T_{ta}}{\partial y^2} = 0 \tag{A2}$$

the solutions take the form:

$$T_{ta} = D'_1 \text{Exp}(\eta s^t \sqrt{Pr}) + D'_2 \text{Exp}(-\eta s^t \sqrt{Pr}) \tag{A3}$$

$$T_{ga} = D_1 \text{Exp}(\eta s^g \sqrt{Pr}) + D_2 \text{Exp}(-\eta s^g \sqrt{Pr}) + T_{\text{ga particular}} \tag{A4}$$

where the constants "D" are determined by verifying the boundaries conditions:

- symmetrical profile of the gas temperature

$$y = 0 \quad \frac{\partial T_{ga}}{\partial y} = 0 \tag{A5}$$

- no temperature jump at wall

$$y = l/2 \quad k_g \frac{\partial T_{ga}}{\partial y} = k_t \frac{\partial T_{ta}}{\partial y} \quad \text{and} \quad T_{ga} = T_{ta} \tag{A6}$$

- possible thermal exchange by convection at the external wall with the surroundings

$$y = l/2 + e_t k_t \quad \frac{\partial T_{ta}}{\partial y} = -h_e T_{ta} \tag{A7}$$

After some tedious calculus, one obtains all the previous constants. They are expressed below introducing several new practical parameters X_i:

$$D_2 = D_1; \quad D'_2 = X_2 D'_1 \tag{A8}$$

with

$$D_1 = -\frac{p_a}{c_g \rho_{g0}} \frac{X_3}{2Ch[s^g\sqrt{Pr}]} \tag{A9}$$

and

$$D'_1 = \frac{2Ch[s^g\sqrt{Pr}]}{X_1} D_1 + \frac{p_a}{X_1 \rho_{gx} c_g}\left(1 + \frac{\Delta_{Tx}}{\Delta_{\text{acou}}}\frac{1}{Pr - 1}\right) \tag{A10}$$

The practical coefficients definitions are

$$X_1 = \text{Exp}[s^t\sqrt{Pr}] + X_2 \text{Exp}[-s^t\sqrt{Pr}] \tag{A11}$$

$$X_{-1} = \text{Exp}[s^t\sqrt{Pr}] - X_2 \text{Exp}[-s^t\sqrt{Pr}] \tag{A12}$$

$$X_2 = -\frac{h_e + k_t \frac{2}{l} s^t \sqrt{Pr}}{h_e - k_t \frac{2}{l} s^t \sqrt{Pr}} \text{Exp}\left[2\left(1 + 2\frac{e_t}{l}\right) s^t \sqrt{Pr}\right] \tag{A13}$$

$$X_3 = \frac{k_t \frac{X_{-1}}{X_1}\sqrt{\frac{a_g}{a_t}}\left(1 + \frac{\Delta_{Tx}}{\Delta_{\text{acou}}}\frac{1}{Pr-1}\right) - k_g \sqrt{\frac{\rho_{gx}}{\rho_{g0}}}\frac{\Delta_{Tx}}{\Delta_{\text{acou}}}\frac{\sqrt{Pr}}{Pr-1} Th[s^g]}{k_t \frac{X_{-1}}{X_1}\sqrt{\frac{a_g}{a_t}} - k_g \sqrt{\frac{\rho_{gx}}{\rho_{g0}}} Th[s^g]} \tag{A14}$$

The latter parameter can be simplified in the case of a gas of weak thermal conductivity in front of the wall conductivity; note also that "X_3" equals to unity for an isothermal wall:

$$X_3 \rightarrow_{k_g/k_t \rightarrow 0} \left(1 + \frac{\Delta_{Tx}}{\Delta_{\text{acou}}}\frac{1}{Pr - 1}\right) \rightarrow_{\Delta_{Tx} \rightarrow 0} 1 \tag{A15}$$

Appendix B

Axial variation of enthalpy flux and second order temperature amplitude Multiplying first order continuity equation by $c_g T_{ga}$, first order movement equation

by u_a, integrating between tangential coordinate and on a period gives

$$c_g\left\langle\int_0^{d/2} T_{ga}\frac{\partial\rho_{ga}}{\partial t}\,dy\right\rangle + c_g\frac{\partial\rho_{gx}}{\partial x}\left\langle\int_0^{d/2} T_{ga}u_a\,dy\right\rangle + c_g\rho_{gx}\left\langle\int_0^{d/2} T_{ga}\frac{\partial u_a}{\partial x}\,dy\right\rangle + c_g\rho_{gx}\left\langle\int_0^{d/2} T_{ga}\frac{\partial v_a}{\partial y}\,dy\right\rangle = 0 \tag{B1}$$

$$\rho_{gx}\left\langle\int_0^{d/2} u_a\frac{\partial u_a}{\partial t}\,dy\right\rangle + \left\langle\int_0^{d/2} u_a\frac{\partial p_a}{\partial x}\,dy\right\rangle + \mu\left\langle\int_0^{d/2} u_a\frac{\partial^2 u_a}{\partial y^2}\,dy\right\rangle = 0 \tag{B2}$$

Integrating second order energy equation with same method,

$$k_g\left\langle\left.\frac{\partial T_{g2a}}{\partial y}\right|_{l/2}\right\rangle = c_g\left\langle\int_0^{d/2}\rho_{ga}\frac{\partial T_{ga}}{\partial t}\,dy\right\rangle + c_g\rho_{gx}\left\langle\int_0^{d/2} u_a\frac{\partial T_{ga}}{\partial x}\,dy\right\rangle + c_g\rho_{gx}\left\langle\int_0^{d/2} v_{ga}\frac{\partial T_{ga}}{\partial y}\,dy\right\rangle - \left\langle\int_0^{d/2} u_a\frac{\partial p_a}{\partial x}\,dy\right\rangle - \mu\left\langle\int_0^{d/2}\left(\frac{\partial u_a}{\partial y}\right)dy\right\rangle \tag{B3}$$

Now substituting terms of the two first equations in the third, one finds

$$k_g\left\langle\left.\frac{\partial T_{g2a}}{\partial y}\right|_{d/2}\right\rangle = c_g\left\langle\int_0^{d/2}\frac{\partial(\rho_{ga}T_{ga})}{\partial t}\,dy\right\rangle + c_g\rho_{gx}\left\langle\int_0^{d/2}\frac{\partial(u_aT_{ga})}{\partial x}\,dy\right\rangle + c_g\rho_{gx}\left\langle\left[v_{ga}T_{ga}\right]_O^{d/2}\right\rangle + \mu\left\langle\int_0^{d/2}\frac{\partial}{\partial y}\left(u_a\frac{\partial u_a}{\partial y}\right)dy\right\rangle + c_g\frac{\partial\rho_{gx}}{\partial x}\left\langle\int_0^{d/2} T_{ga}u_a\,dy\right\rangle = \frac{\partial}{\partial x}\langle\dot{h}_x\rangle \tag{B4}$$

This equation leads to a simple explanation: permanent part of the second order temperature perturbation increases the lateral thermal exchanges which are responsible of the axial variation of the energy flux.

Appendix C

For classic external rectangular fins in free ambience, the efficiency is

$$\eta_a' = -\frac{k_f S\left(\left.\frac{\partial T}{\partial y}\right|_{y=d}\right)}{h\Sigma_a(T|_{y=0} - T_g)} = \frac{mk_fS}{h\Sigma}\frac{Sh[ml] + \frac{h}{mk_f}Ch[ml]}{Ch[ml] + \frac{h}{mk_f}Sh[ml]} \tag{C1}$$

with

$$m^2 = \frac{hp}{k_fS} \quad S = e_f l_0 \quad p = 2(e_f + l_0) \quad \Sigma_a = l(e_f + l_0) \tag{C2}$$

So we deduce a weighted factor for surface with slabs.

$A = Ne_f l_0$ is the finned area (C3)

$B = (1+N)(d_f - e_f)l_0$ is the area without fins (C4)

$\Sigma = Nl(e_f + l_0)$ is the external half surface of fins (C5)

Thermal flux exchanged between the fluid and the finned walls $\dot{Q}$ and the thermal flux exchangeable with both walls without fins $\dot{Q}^*$, are respectively:

$$\dot{Q} = h(B + \eta_a\Sigma)(T_0 + T_l - 2T_g) \tag{C6}$$

$$\dot{Q}^* = h(A+B)(T_0 + T_l - 2T_g) \tag{C7}$$

So the weighted factor to take into account of the finned area is

$$\eta_s = \frac{\dot{Q}}{\dot{Q}^*} = \frac{B}{A+B} + \eta_a\frac{\Sigma}{A+B} \tag{C8}$$

References

[1] R. Shekarriz, C.J. Call, State of the art in micro and meso scale heat exchangers, proceedings of the ASME, Adv. Energy Syst. Division AES-Vol 39 (1999) 5361.

[2] A.A. Rostami, A.S. Mujumdar, N. Saniei, Flow and heat transfer for gas flowing in microchannels: a review, Heat Mass Transfer (2001).

[3] Y. Bailly, Ph. Nika, M. De Labachelerie, J.C. Jeannot, J. De Lallée, Vers la miniaturisation d'une machine frigorifique de type Tube à Gaz Pulsé, Congrès Français de Thermique, 29–31 mai, Nantes, 2001.

[4] C. Aubert, Ecoulements compressibles de gaz dans les microcanaux: effets de raréfaction, effets instationnaires, Thèse de L' Université Paul Sabatier, n°3349, 1999.

[5] C. Aubert, S. Colin, High-order boundary conditions for gaseous flows in rectangular microducts, Microscale Thermophys. Eng. 5 (2001) 41–54.

[6] G. Tunc, Y. Bayazitoglu, Heat transfer in rectangular microchannels, Int. J. Heat Mass Transfer 45 (2002) 765–773.

[7] C.Y. Zhao, T.J. Lu, Analysis of microchannel heat sinks for electronics cooling, Int. J. Heat Mass Transfer 45 (2002) 4857–4869.

[8] C.L. Tien, G. Chen, Challenges in microscale conductive and radiative heat transfer, J. Heat Transfer 116 (November) (1994) 799–806.
[9] D. Gedeon, Mean parameter modeling of oscillating flow, J. Heat Transfer 108 (August) (1986) 513–518.
[10] Dae-Young Lee, Sang-Jin Park, Sung Tack Ro, Heat transfer by oscillating flow in circular pipe with a sinusoidal wall temperature distribution, Int. J. Heat Mass Transfer 38 (14) (1995) 2529–2537.
[11] Dae-Young Lee, Sang-Jin Park, Sung Tack Ro, Heat transfer in the thermally developing region of a laminar oscillating pipe flow, Cryogenics 38 (1998) 585–594.
[12] A.A. Khornauser, J.L. Smith, Application of a complex Nusselt number to heat transfer during compression and expansion, Trans. ASME 116 (August) (1994) 536–542.
[13] H. Schilichting, Boundary layer theory, seventh ed., McGrawHill, New York, 1979.
[14] Y. Fang, Numerical simulations of high Knudsen number gas flows and microchannel electrokinetic liquid flows, thesis of Drexel University, 2003.
[15] P. Nika, Y. Bailly, F. Lanzetta, Transferts thermiques en écoulements alternés, Int. J. Refrigerat., in press.
[16] G.W. Swift, Thermoacoustics: a unifying perspective for some engines and refrigerators, Fifth draft LA UR 99 895 29 May 2001.
[17] G.W. Swift, Thermoacoustic engines and refrigerators, Phys. Today (July) (1995) 22–28.
[18] J. Wheatley, T. Hofler, G.W. Swift, A. Migliori, Understanding some simple phenomena in thermoacoustics with applications to acoustical heat engines, Am. J. Phys. 53 (2) (1985) 147–162.
[19] G.W. Swift, Thermoacoustic engines, J. Acoust. Soc. Am. 84 (4) (1988), October.
[20] N. Rott, Thermoacoustics, Adv. Appl. Mech. 20 (1980) 135–174.
[21] J.H. Xiao, Thermoacoustic heat transportation and energy transformation Part 1, 2, 3, Cryogenics 35 (1995) 15–29.
[22] F.W. Giacobbe, Heat transfer capability of selected binary gaseous mixtures relative to helium and hydrogen, Appl. Thermal Eng. 18 (3–4) (1998) 199–206.
[23] P.X. Jiang, M.H. Fan, G.S. Si, Z.P. Ren, Thermal-hydraulic performance of small scale micro-channel and porous-media heat exchangers, Int. J. Heat Mass Transfer 44 (2001) 1039–1051.
[24] Y. Bailly, P. Nika, Comparison of two models of a double inlet miniature pulse tube refrigerator: part B electrical analogy, Cryogenics 42 (2002) 605–615.